

Title	Methylcelluloses end-functionalized with peptides as thermoresponsive supramolecular hydrogelators
Author(s)	Suhara, Ryo; Yamagami, Mao; Kamitakahara, Hiroshi; Yoshinaga, Arata; Tanaka, Yoshimasa; Takano, Toshiyuki
Citation	Cellulose (2019), 26(1): 355-382
Issue Date	2019-01
URL	http://hdl.handle.net/2433/242287
Right	This is a post-peer-review, pre-copyedit version of an article published in Cellulose. The final authenticated version is available online at: http://dx.doi.org/10.1007/s10570-018-2027-5 .; This is not the published version. Please cite only the published version. この論文は出版社版ではありません。引用の際には出版社版をご確認ご利用ください。
Type	Journal Article
Textversion	author

1 **Methylcelluloses End-Functionalized with**
2 **Peptides as Thermoresponsive**
3 **Supramolecular Hydrogelators**

4

5 Ryo Suhara[†], Mao Yamagami[†], Hiroshi Kamitakahara^{*†}, Arata Yoshinaga[†],
6 Yoshimasa Tanaka[§], Toshiyuki Takano[†]

7 [†]*Graduate School of Agriculture, Kyoto University, Kitashirakawa-Oiwake-cho,*
8 *Sakyo-ku, Kyoto 606-8502, Japan*

9 [§]*Center for Bioinformatics and Molecular Medicine, Graduate School of*
10 *Biomedical Sciences, Nagasaki University, 1-12-4 Sakamoto, Nagasaki 852-8523,*
11 *Japan*

12

13 AUTHOR INFORMATION

14 **Corresponding Author:** Hiroshi Kamitakahara

15 *E-mail: hkamitan@kais.kyoto-u.ac.jp; Tel: +81-75-753-6257

16 ORCID: Hiroshi Kamitakahara: 0000-0002-0130-1919

17

18 **Abstract** This paper describes the synthesis of methylcelluloses end-
19 functionalized with peptides and an investigation into their functions. We found
20 that aqueous solutions of methylcellulose end-functionalized not only with
21 carbohydrates but also with peptide segments, such as di(arginine) and
22 di(glutamic acid), behave as thermoresponsive supramolecular hydrogelators at
23 human-body temperature. The slow drug release from thermoresponsive
24 hydrogels of methylcelluloses end-functionalized with peptides is attributed to
25 ionic interactions between model drugs and peptide segments in these hydrogels.
26 Reactions of methylated cellobiose with di(arginine) and di(glutamic acid) were
27 used to determine optimum reaction conditions for the synthesis of
28 methylcelluloses end-functionalized with these peptide residues). The surface
29 activities, zeta potentials, thermal properties, hydrogelation behavior, and
30 cytotoxicities of these peptide-functionalized methylcelluloses are also discussed.

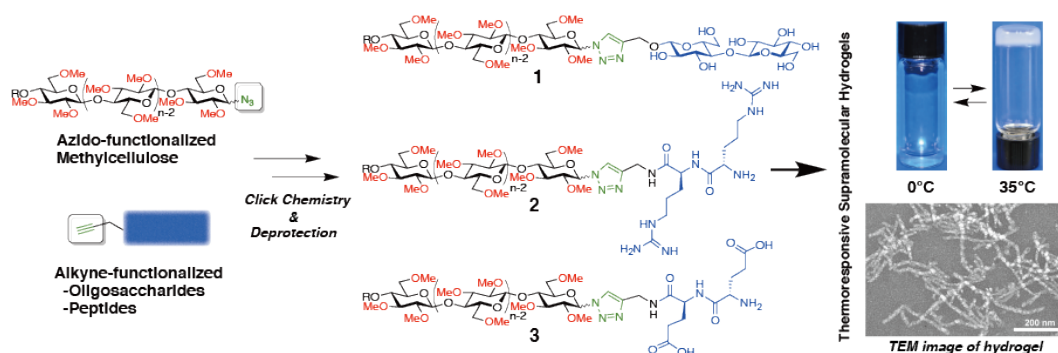
31

32 **Highlights:**

- 33 • Methylcelluloses end-functionalized with peptides were synthesized.
- 34 • Peptides-end-functionalized methylcelluloses behave as thermoresponsive
- 35 supramolecular hydrogelators at human-body temperature.
- 36 • The slow drug release from thermoresponsive hydrogels of methylcelluloses
- 37 end-functionalized with peptides was achieved.

38

39 **Graphical Abstract:**



40

41

42 **Introduction**

43 Thermoresponsive hydrogels have received increased attention in recent years.
44 In particular, thermoresponsive supramolecular hydrogels (Du et al. 2015) with
45 lower critical solution temperatures (LCSTs) (Yamagami et al. 2018) enable the
46 development of biomedical applications such as injectable drug-delivery
47 technology (Baumann et al. 2009). While poly(*N*-isopropylacrylamide)
48 (Fundueanu et al. 2009) is a well known thermoresponsive polymer derived from
49 fossil resources, methylcellulose (MC) is a thermoresponsive material from
50 renewable resources.

51 The degree of substitution (DS) of industrially produced MC is 1.8, and its
52 aqueous solution exhibits thermoreversible hydrogelation at approximately 60 °C.
53 The physical properties of aqueous MC solutions have received considerable
54 academic attention (Desbrieres et al. 1998; Heymann 1935; Rees 1972; Savage
55 1957). Kato et al. concluded that the network junction points in MC gels are
56 between 4 and 8 units long (Kato et al. 1978).

57 Our studies have focused on structure-property-function relationships of
58 methylcellulose (Kamitakahara et al. 2009a; Kamitakahara et al. 2009b;
59 Kamitakahara et al. 2008a; Kamitakahara et al. 2012; Kamitakahara and
60 Nakatsubo 2010; Kamitakahara et al. 2006; Kamitakahara et al. 2007;
61 Kamitakahara et al. 2009c; Kamitakahara et al. 2008b; Karakawa et al. 2002;
62 Nakagawa et al. 2011a; Nakagawa et al. 2011b; Nakagawa et al. 2012a;
63 Nakagawa et al. 2012b; Nakagawa et al. 2012c). Diblock methylcellulose bearing
64 a sequence of at least ten 2,3,6-tri-*O*-methylglucosyl units and an unmodified
65 cellobiosyl unit plays a crucial role in the thermoreversible hydrogelation of an
66 aqueous MC solution (Nakagawa et al. 2011a).

67 Our detailed study on the structure-property relationships of methylcellulose
68 with a sequence of over twenty 2,3,6-tri-*O*-methylglucosyl units revealed the
69 thermoreversible hydrogelation properties of an aqueous diblock methylcellulose
70 solution at human-body temperature (Nakagawa et al. 2011a). In addition, Bodvik
71 et al. reported that MC forms fibrillar aggregates that were observed by cryogenic
72 transmission electron microscopy (Cryo-TEM) (Bodvik et al. 2010); we also
73 reported the same morphology (Nakagawa et al. 2012c), as did the group of
74 Lodge (Lott et al. 2013a; Lott et al. 2013b). Moreover, we found that well-defined
75 diblock methylcellulose self-assembles thermoresponsively into ribbon-like
76 nanostructures in water to form a thermoreversible hydrogel at human-body
77 temperature (Nakagawa et al. 2012c). The intermolecular interactions in the
78 fibrillar nanostructure of commercial MC in aqueous solution at LCST and in the
79 ribbon-like nanostructure of well-defined diblock methylcellulose are essentially
80 the same; hydrophobic interactions between a sequence of 2,3,6-tri-*O*-
81 methylglucosyl units, and hydrogen bonding between less-methylated glucosyl
82 units both play crucial roles during the aggregation of methylcellulose molecules
83 at LCST.

84 This finding prompted us to explore methylcellulose analogues that can be
85 synthesized by more simple and straightforward methods than glycosylation
86 (Nakagawa et al. 2011b). We selected the Huisgen 1,3-dipolar cycloaddition
87 reaction for the development of methylcellulose analogues (Nakagawa et al.
88 2012b). An aqueous solution of the newly synthesized methylcellulose analogue,
89 which included hydrophobic and hydrophilic segments connected by 1,2,3-
90 triazoles, exhibited thermoreversible hydrogelation properties (Nakagawa et al.
91 2012b) equivalent to that of a well-defined diblock methylcellulose (Nakagawa et
92 al. 2011b). Consequently, we developed a synthetic method for the end-

93 functionalization of methylcellulose to produce methylcellulosyl azide and
94 propargyl methylcelluloside (Kamitakahara et al. 2016). Moreover, not only did
95 nonionic segments, such as cellobiosyl units (as hydrophilic blocks) induce
96 thermoreversible hydrogelation, but ionic segments did as well (Yamagami et al.
97 2018), although it was crucial that the concentrations of the diblock
98 methylcellulose analogues in aqueous media remain at 4 wt%.

99 Our recent results suggested that it might be possible to install any functional
100 group at the methylcellulose end and retain thermoreversible hydrogelation
101 behavior at human-body temperature. Hence, we explored the end-
102 functionalization of methylcellulose with peptides. Peptides exhibit potent
103 biological activities due to the functional diversity of their amino-acid chains, and
104 play crucial roles in organisms that differ from those of oligo- and
105 polysaccharides. Therefore, the end-functionalizations of polysaccharide
106 derivatives with peptides are expected to yield a variety of functional materials
107 that exhibit thermoresponsive properties. An oligosaccharide-based synthetic
108 glycoprotein (Bonduelle and Lecommandoux 2013) has been reported by the
109 group of Lecommandoux. However, polysaccharide-derivative-*block*-
110 oligosaccharides (Breitenbach et al. 2017; de Medeiros Modolon et al. 2012) or
111 polysaccharide-derivative-*block*-oligopeptides have not received much attention
112 from researchers. Carbohydrate-based block copolymers with polyester (Fajardo
113 et al. 2014; Liu and Zhang 2007), poly(methyl methacrylate) (Dax et al. 2013;
114 Togashi et al. 2014), poly(styrene) (Loos and Müller 2002; Otsuka et al. 2013;
115 Yagi et al. 2010), poly(*N*-isopropylacrylamide) (Dax et al. 2013; Otsuka et al.
116 2012), poly(γ -benzyl-L-glutamate) (Kamitakahara et al. 2014), and poly(3-
117 hexylthiophene) (Sakai-Otsuka et al. 2017) polyisoprene (Hung et al. 2017), and
118 poly(ethyleneoxide) (Akiyoshi et al. 1999) have been reported. Shoichet and her

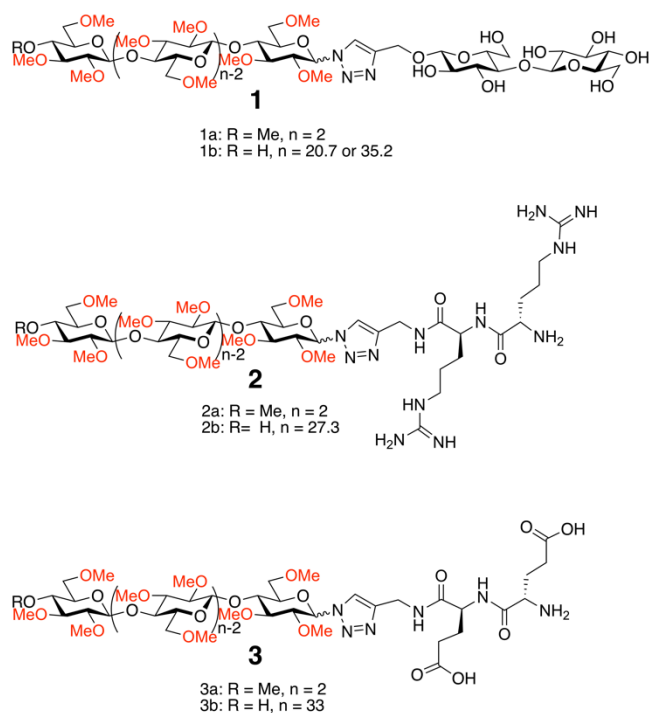
119 colleagues focused on a physical blend of hyaluronan and methylcellulose
120 covalently linked to peptides for tissue-engineering purposes (Parker et al. 2016).
121 They modified methylcellulose with peptides by the "grafting to" method, in
122 which peptide moieties were randomly introduced onto the methylcellulose
123 backbone. In contrast, our method gives thermoresponsive hydrogels composed of
124 only methylcellulose and peptides, and are devoid of other polysaccharides. Our
125 new peptide-end-functionalized methylcelluloses are linear polysaccharide
126 derivatives with blocky structures that exhibit a broad range of new properties,
127 including thermoreversible hydrogelation at temperatures close to that of the
128 human body, formation of ribbonlike supramolecular nanostructures by self-
129 assembly, surface activities, and slow drug release from thermoresponsive
130 supramolecular hydrogel.

131 Herein, we describe the end-functionalization of tri-*O*-methylcellulose with
132 cationic di(arginine) and anionic di(glutamic acid) units as peptide segments in
133 order to develop new functionality (Chart 1). The synthesis, characterization, and
134 thermal properties of aqueous solutions of these materials, as well as their zeta
135 potentials, surface activities, in vitro cytotoxicities, and drug-release behavior
136 from their supramolecular hydrogel matrices, are discussed.

137

138

139 **Chart 1. Compounds 1–3.**



140

141

142 **Results and discussion**

143 **Synthesis of Peptide Segments**

144 Peptide segments were synthesized following standard Fmoc methodology, as
145 shown in Scheme 1. For side-chain protection, we used the 2,2,4,6,7-
146 pentamethyldihydrobenzofuran-5-sulfonyl (pbf) group for the guanidine group,
147 while the γ carboxylic acid group of glutamic acid was protected as a *tert*-butyl
148 (*t*Bu) ester.

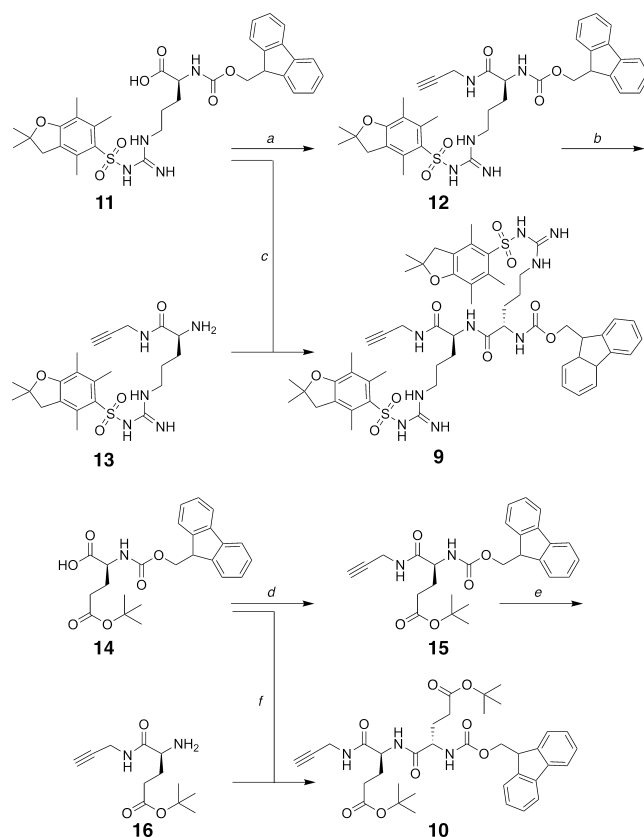
149 Propargylamine was reacted with *N* α -Fmoc-*N* ω -Pbf-L-arginine (**11**) to give the
150 alkyne-functionalized *N* α -Fmoc-*N* ω -Pbf-L-arginine-*N*-propargylamide (**12**) in
151 89% yield. The amide bond was successfully formed with DMT-MM (Kunishima
152 et al. 1999a; Kunishima et al. 1999b) as the condensation reagent. The Fmoc
153 group of compound **12** was removed to afford *N* ω -Pbf-L-arginine-*N*-

154 propargylamide (**13**) in 82% yield. *N*α-Fmoc-*N*ω-Pbf-L-arginine (**11**) was
 155 coupled with *N*ω-Pbf-L-arginine-*N*-propargylamide (**13**) to produce *N*α-Fmoc-
 156 *N*ω-Pbf-L-arginine-*N*ω-Pbf-L-arginine-*N*-propargylamide (**9**) in 89% yield.

157 Fmoc-Glu(*O**t*-Bu)-OH (**14**) was also reacted with propargylamine to produce
 158 the alkyne-functionalized Fmoc-Glu(*O**t*-Bu)-*N*-propargylamide (**15**) in
 159 quantitative yield. Removal of the Fmoc group from compound **15** afforded
 160 Glu(*O**t*-Bu)-*N*-propargylamide (**16**) in quantitative yield. Compounds **14** and **16**
 161 were coupled with DMT-MM to produce *N*α-Fmoc-Glu(*O**t*-Bu)-Glu(*O**t*-Bu)-*N*-
 162 propargylamide (**10**) in 95% yield.

163 Compounds **9** and **10**, bearing alkyne groups, are peptide-containing segments
 164 for the end-functionalization of methylcellulose.

165

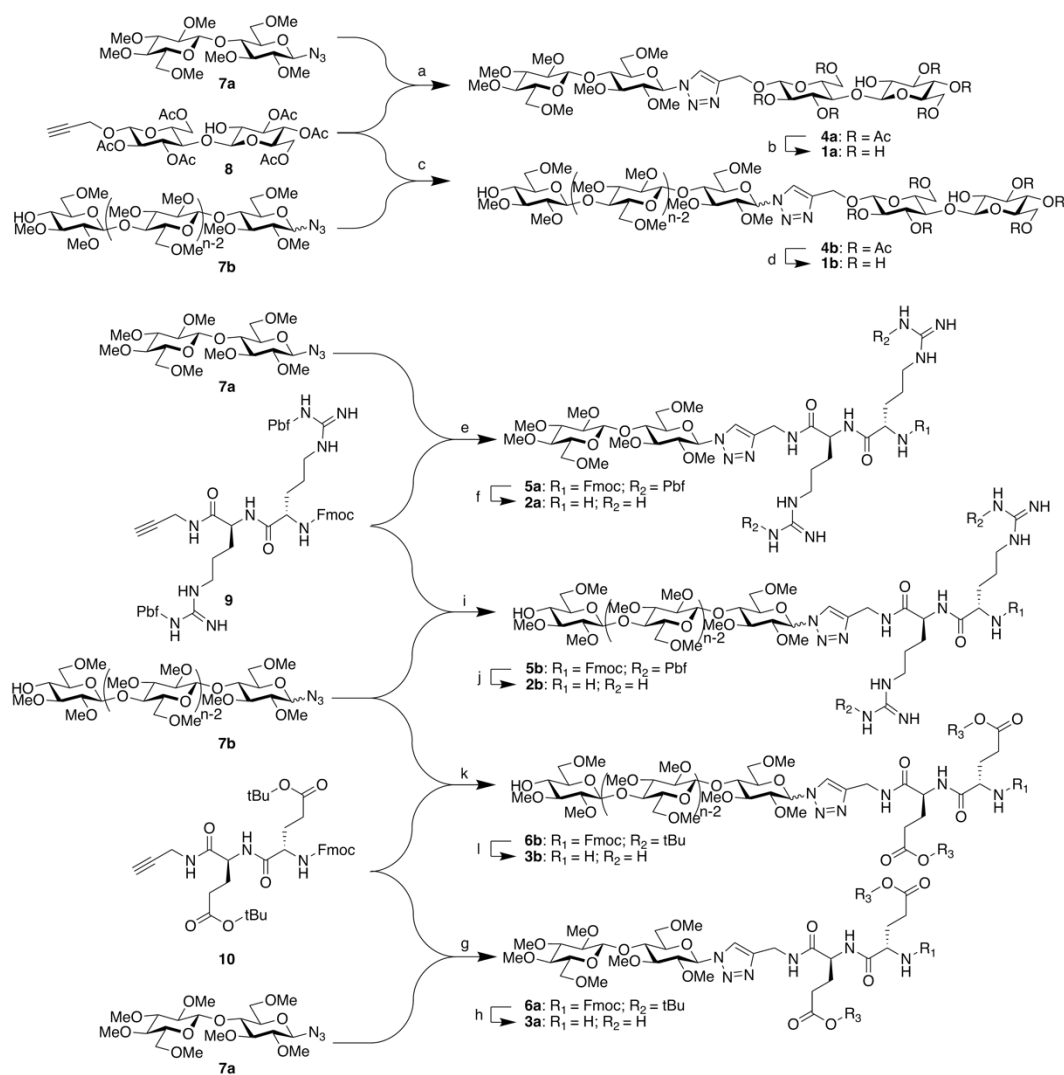


166 **Scheme 1.** Synthesis of peptide segments **9** and **10**. (a) propargylamine / DMT-MM / MeOH / r.t. /
 167 3 h / 89%; (b) piperidine/CH₂Cl₂ / r.t. / 1 / 82%; (c) DMT-MM / MeOH / r.t. / 4 h / 89%; (d)
 168 propargylamine / DMT-MM / MeOH / r.t. 3 h / quantitative yield; (e) piperidine/CH₂Cl₂ / r.t. / 1 h
 169 / quantitative yield; (f) DMT-MM / MeOH / r.t. / 1 h / 95%.

170

171 **Peptide-End-Functionalized Methylcelluloses by Huisgen 1,3-Dipolar**
172 **Cycloadditions**

173 Scheme 2 displays the synthetic routes to methylcelluloses end-functionalized
174 with peptides, as well as the control compounds. Trehalose-type methylated
175 cellobiose derivative **1a** and diblock methylcellulose analogues **1b** (Yamagami et
176 al. 2018) are control compounds for peptide-functionalized methylated cellobiose
177 derivatives **2a** and **3a**, and peptide-end-functionalized methylcelluloses **2b** and **3b**,
178 respectively.



179
180

Scheme 2. Synthesis of methylcelluloses end-functionalized with peptides

181 a) Cu(I)Br / sodium ascorbate / PMDETA / DMF / r.t. / 21 h / 56%; b) 28% NaOCH₃ in MeOH /
182 MeOH/THF / r.t. / 3 h / quantitative yield; c) CuBr / sodium ascorbate / PMDETA /
183 MeOH/CH₂Cl₂ / r.t. / 4 d / 78.5%; d) 28% NaOCH₃ in MeOH / MeOH/THF / r.t. / overnight /
184 quantitative yield; e) Cu(I)Br / sodium ascorbate / MeOH/CH₂Cl₂ / r.t. / 2 h / 85%; f) piperidine /

185 CH₂Cl₂ / r.t. / 1 h / 65%; TFA/H₂O / 37 °C / 4 h / 52%; g) CuBr / sodium ascorbate / MeOH /
186 CH₂Cl₂ / r.t. / 2 h / 87%; h) piperidine / CH₂Cl₂ / r.t. / 1 h / 47%; TFA/H₂O / r.t. / 4 h / 58%; i)
187 CuSO₄·H₂O / sodium ascorbate / MeOH/CH₂Cl₂ / r.t. / 14 h / quantitative yield; j)
188 piperidine/CH₂Cl₂ / r.t. / 4 h / 89%; TFA/H₂O / 37 °C / 4 h / 76%; k) CuSO₄·H₂O / sodium ascorbate
189 / MeOH/CH₂Cl₂ / r.t. / 14 h / 93%; l) piperidine/CH₂Cl₂ / r.t. / 4 h / 84%; TFA/H₂O / r.t. / 4 h / 52%.

190

191 Methylated cellobiose derivatives **2a** and **3a** were prepared in order to optimize
192 reaction conditions for the methylcellulose derivatives. Copper-assisted azide-
193 alkyne cycloaddition (CuAAC, the “click reaction”) of 2,3,4,6-tetra-*O*-methyl-β-
194 D-glucopyranosyl-(1→4)-2,3,6-tri-*O*-methyl-β-D-glucopyranosyl azide (**7a**) and
195 propargylated peptide segments **9** and **10** afforded methylated cellobiose
196 derivatives **5a** (85% yield) and **6a** (87% yield) bearing peptide residues,
197 respectively. Subsequent deprotections of the peptide segments gave methylated
198 cellobioses **2a** and **3a** end-functionalized with peptides.

199 The optimized reaction conditions for the cellobiose derivatives allowed us to
200 synthesize the peptide-functionalized methylcelluloses **2b** and **3b**. The CuAAC
201 reactions of tri-*O*-methylcellulosyl azide (**7b**) and propargylated peptide segments
202 **9** and **10** afforded methylcelluloses **5b** and **6b** end-functionalized with protected
203 peptides, respectively; deprotection of the peptide segments of these compounds
204 afforded peptide-functionalized methylcelluloses **2b** and **3b**.

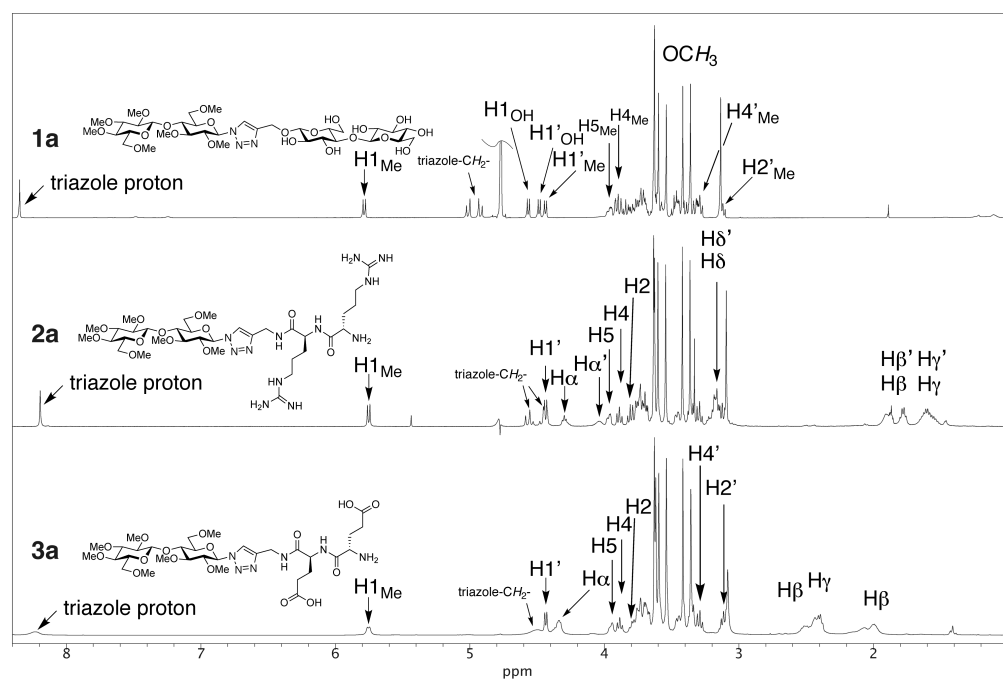
205 While tri-*O*-methylcellulosyl azide (**7b**) is a mixture of both α- and β-anomers,
206 the cellobiosyl azide **7a** is only the β-anomer. Moreover, each methylcellulose
207 derivative **7b**, **4b**, **5b**, **6b**, **1b**, **2b**, and **3b** bears a single hydroxyl group at the C-4
208 position of its methylated glucosyl residue furthest from the azide. In contrast,
209 cellobiosyl azide derivative **7a** has no such hydroxyl group. We have reported the
210 synthesis of blockwise alkylated (1→4) linked trisaccharides, and found that the
211 anomeric configuration between the hydrophobic and hydrophilic segments
212 affects surface activity of the aqueous solution (Nakagawa et al. 2011c).

213

214 **Characterization**

215 Figure 1 displays the ^1H -NMR spectra of cellobiose derivatives **1a**, **2a**, and **3a**
216 acquired in deuterium oxide. Proton resonances are assigned on the basis of two-
217 dimensional NMR experiments (see experimental section). The triazole protons of
218 compounds **1a**, **2a**, and **3a** appear at 8.24, 8.19, and 8.24 ppm, respectively.
219 Carbon resonances of compounds **1a**, **2a**, and **3a** have also been assigned (see
220 experimental section). Interestingly, the triazole proton of compound **3a** appears
221 as a broad singlet. The methylene protons of compound **3a** adjacent to the triazole
222 ring also appear as a broad peak at about 4.40–4.61 ppm. In addition, the C-1
223 proton of the cellobiosyl residue appears as a broad doublet at 5.75 ppm.

224 The transverse relaxation times $T_2\text{s}$ of triazole proton and C1 proton adjacent to
225 the triazole of anionic compound **3a** would be shorter than that of compounds **1a**
226 and **2a**, although molecular weights of compounds **1a**, **2a**, and **3a** are similar. The
227 transverse relaxation times $T_2\text{s}$ of protons of an anionic surfactant, sodium
228 dodecyl sulfate (SDS), depend on their positions; $T_2\text{s}$ of the internal protons are
229 shorter than that of methyl protons and methylene protons adjacent to the sulfate
230 group (Yu et al. 2017). The transverse relaxation time $T_2\text{s}$ of the protons of
231 anionic compound **3a** showed the same tendency as the anionic surfactant, SDS.



232

233 **Figure 1.** 500-MHz $^1\text{H-NMR}$ spectra of compounds **1a**, **2a**, and **3a** in D_2O .

234

235 Figure 2 displays the MALDI-TOF MS spectra of compounds **1a**, **2a**, and **3a**.

236 Pseudomolecular sodium $[\text{M}+\text{Na}]^+$ and potassium $[\text{M}+\text{K}]^+$ adduct-ion peaks

237 corresponding to compound **1a** appear at m/z 868.6 and 884.6, respectively. The

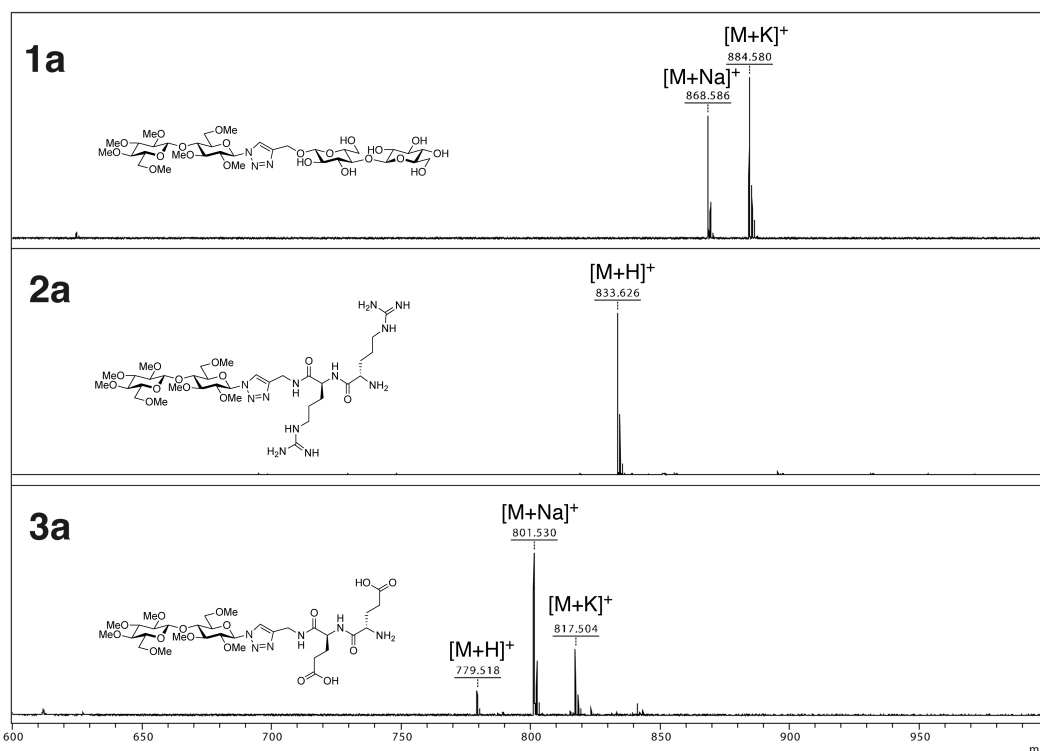
238 pseudomolecular proton adduct-ion peak $[\text{M}+\text{H}]^+$ of compound **2a** appears at m/z

239 833.6, while pseudomolecular proton $[\text{M}+\text{H}]^+$, sodium $[\text{M}+\text{Na}]^+$, and potassium

240 $[\text{M}+\text{K}]^+$ adduct-ion peaks of compound **3a** appear at m/z 779.5, 801.5, and 817.5,

241 respectively.

242

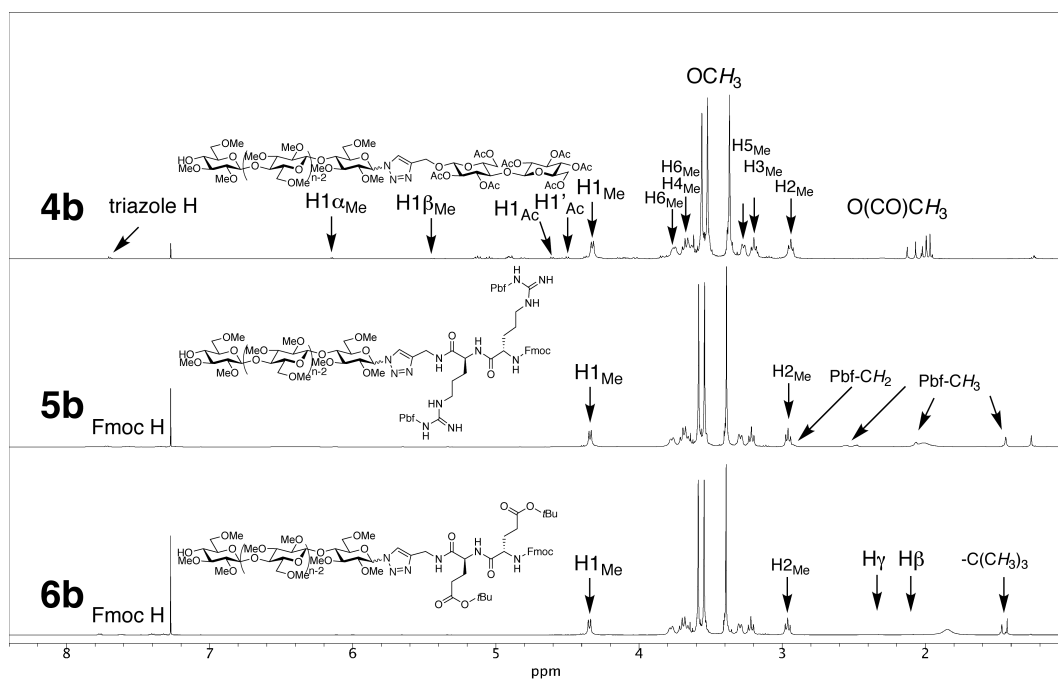


243

244 **Figure 2.** MALDI-TOF MS spectra of compounds **1a**, **2a**, and **3a**.

245

246 In summary, the NMR and MALDI-TOF MS data for cellobiose derivatives **1a**,
 247 **2a**, and **3a** reveal that the conditions for the CuAAC reactions and the
 248 deprotections of the peptide residues are appropriate. Hence, the reaction
 249 conditions developed for these cellobiose derivatives were used to synthesize the
 250 peptide-functionalized methylcelluloses **1b**, **2b**, and **3b**.



251

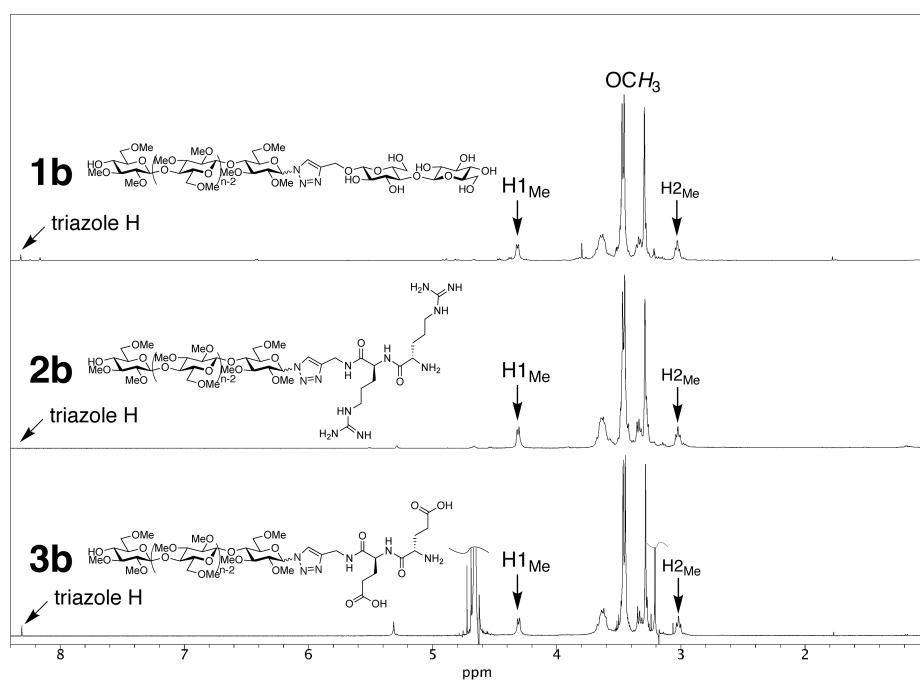
252 **Figure 3.** $^1\text{H-NMR}$ spectra of compounds **4b**, **5b**, and **6b** in CDCl_3 .

253

254 Compounds **5b** and **6b** as well as the trehalose-type diblock methylcellulose
 255 analogue **4b** (Yamagami et al. 2018), as an authentic sample of a methylcellulose
 256 end-functionalized with a peptide, were synthesized according to the optimized
 257 reaction conditions for cellobiose derivatives **5a** and **6a**, as well as **4a**. Figure 3
 258 displays the $^1\text{H-NMR}$ spectra of compounds **4b**, **5b**, and **6b** acquired in CDCl_3 .
 259 The triazole proton of compound **4b** appears at 7.69 (β -anomer) and 7.70 (α -
 260 anomer) ppm (α/β ratio = 2/1) (Yamagami et al. 2018), while the triazole protons
 261 of compounds **5b** and **6b** were unable to be identified due to overlapping
 262 resonances associated with the aromatic protons of their Fmoc groups, although
 263 proton resonances of the peptide side-chains were observed.

264 The same deprotection procedures used for the cellobiosyl compounds **1a**, **2a**,
 265 and **3a** were used for the polymeric compounds, to give methylcellulose
 266 derivatives **1b**, **2b**, and **3b**. Figure 4 displays the $^1\text{H-NMR}$ spectra of

267 methylcellulose derivatives **1b**, **2b**, and **3b** acquired in D₂O. Resonances
268 corresponding to the peptide moieties at the methylcellulose ends are not clearly
269 evident in their spectra because of the higher DP of the methylcellulose residues,
270 compared to the cellobiosyl compounds **1a**, **2a**, and **3a**, as shown in Figure 1.
271 However, the triazole protons of compounds **2b** and **3b** appear at 8.42 and 8.43
272 ppm, respectively, although those of compound **1a** appear at 8.42, 8.35, and 8.27
273 ppm. This fact indicates that compounds **2b** and **3b** are end-functionalized with
274 peptide residues. The zeta potential of compounds **1b**, **2b**, and **3b** summarized in
275 Table 1 also indicate that the deprotections of compounds **2b** and **3b** were
276 successful.
277

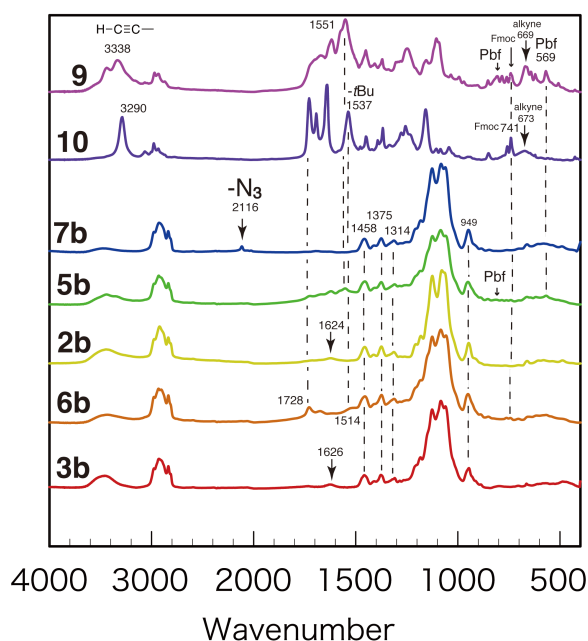


278 **Figure 4.** ¹H-NMR spectra of compounds **1b**, **2b**, and **3b** in D₂O.

279

280 Figure 5 displays the FT-IR spectra of compounds **2b**, **3b**, **5b**, **6b**, **7b**, **9**, and **10**.
281 Infrared absorption peaks corresponding to the protected di(arginine) and
282 di(glutamic acid) segments **9** and **10** appear in the spectra of methylcelluloses **5b**

283 and **6b** end-functionalized with the di(arginine), and di(glutamic acid) derivatives,
284 respectively. The infrared absorption peak associated with methylcellulosyl azide
285 **7b** was observed at 2116 cm^{-1} . After the Huisgen 1,3-dipolar cycloaddition of **7b**
286 with the di(arginine) or di(glutamic acid) derivatives **9** or **10**, infrared absorption
287 peaks associated with the azido group were not evident in the spectra of **5b** and **6b**,
288 which indicates that the Huisgen 1,3-dipolar cycloadditions were successful. The
289 infrared spectra of compounds **5b** and **6b** changed during deprotection to give **2b**
290 and **3b**. The infrared absorption peaks corresponding to Pbf and Fmoc groups of
291 MC-*b*-(Arg(Pbf))₂-Fmoc **5b** were not evident in the spectrum of MC-*b*-ArgArg **2b**.
292 The infrared absorption peaks associated with the *t*Bu and Fmoc groups of MC-*b*-
293 (Glu(O*t*Bu))₂-Fmoc **6b** were not evident in the spectrum of MC-*b*-GluGlu **3b**. The
294 FT-IR analyses of the end-functionalized methylcellulose derivatives provide us
295 with additional experimental data regarding the polymer reactions that occur at the
296 ends of these macromolecules. We conclude that methylcelluloses **2b** and **3b** end-
297 functionalized with peptides were successfully synthesized.



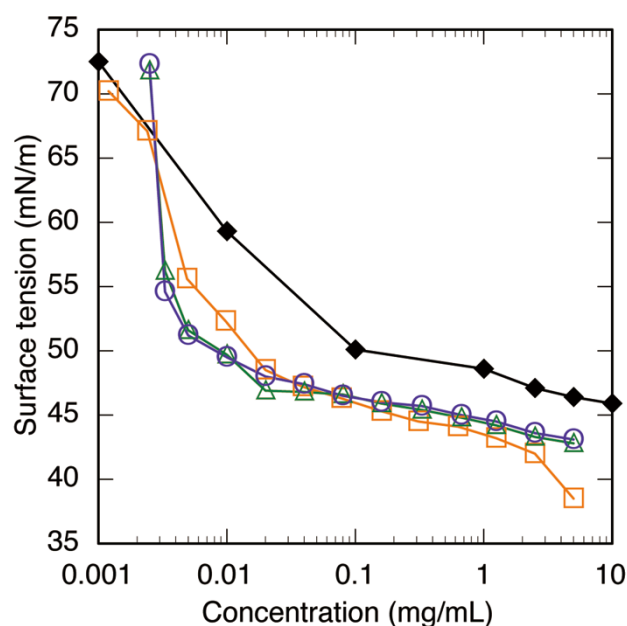
298

299 **Figure 5.** FT-IR spectra of compounds **2b**, **3b**, **5b**, **6b**, **7b**, **9**, and **10**.

300

301 **Physical properties of compounds 1b, 2b, and 3b**

302 Table 1 summarizes the structures, solution surface tensions, and zeta potentials
303 of compounds **1b**, **2b**, and **3b**, while Figure 6 shows the surface tensions of
304 solutions of compounds **1b**, **2b**, and **3b** as functions of concentration, measured at
305 23 °C. Compounds **2b** and **3b** exhibited similar surface-tension curves; the critical
306 micelle concentrations (CMCs) of the arginine-containing compound **2b** and the
307 glutamic-acid-containing compound **3b** are both 0.0035 mg/mL, slightly lower
308 than that of the cellobiose derivative **1b** (0.008 mg/mL). An ionic peptide residue
309 at the end of the methylcellulose unit improves its surface activity compared to
310 that of methylcellulose end-functionalized with the nonionic cellobiosyl residue.
311 In contrast, the CMCs of methylcelluloses **2b** and **3b** end-functionalized with
312 peptides (0.0035 mg/mL) are clearly lower than that of commercial SM-4
313 methylcellulose (0.1 mg/mL).



314 **Figure 6.** Surface tensions of compounds **1b**, (orange open squares), **2b** (green open triangles),
315 and **3b** (purple open circles), and commercial MC (black solid diamonds), as functions of
316 concentration.

317

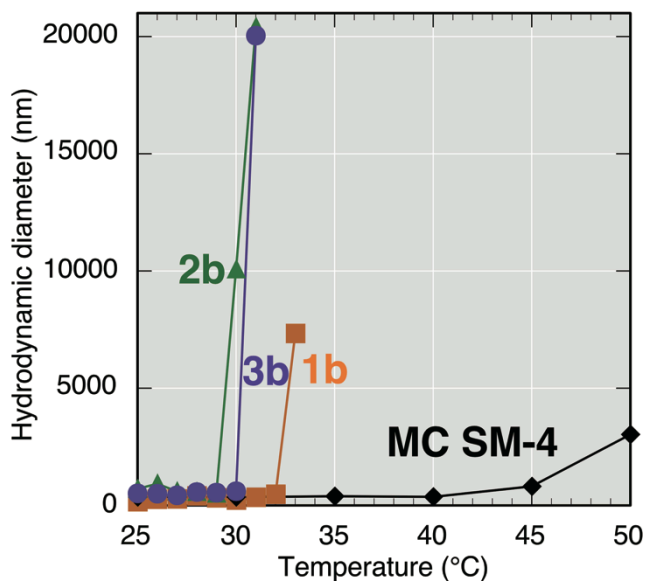
318 **Table 1.** Surface tensions and zeta potentials of compounds **1b**, **2b**, and **3b**.

Comp. No.	Hydrophilic segment	DP_n of hydrophobic segment	DS	Surface tension (mN/m) at CMC	Critical micelle concentration (mg/mL)	Zeta potential (mV)
MC			1.8	50.1	0.1	
1b	Cellobiose	20.7	2.65	49.0	0.008	-11.5
2b	Arginine dimer	27.3	–	47.3	0.0035	-7.5
3b	Glutamic acid dimer	32.8	–	49.3	0.0035	-14.1

319

320 Figure 7 displays the temperature-dependence of the supramolecular
321 aggregation behavior of compounds **1b**, **2b**, and **3b** in water, obtained by dynamic
322 light scattering (DLS) experiments. The hydrodynamic diameters of compounds
323 **1b**, **2b**, and **3b** at 25 °C were determined to be 138, 706, and 476 nm, respectively.
324 Although the hydrodynamic diameter of commercial MC SM-4 gradually
325 increased at temperatures above approximately 45 °C, those of compounds **1b**, **2b**,
326 and **3b** increased dramatically at 33 °C, 30 °C, and 31 °C, respectively.

327

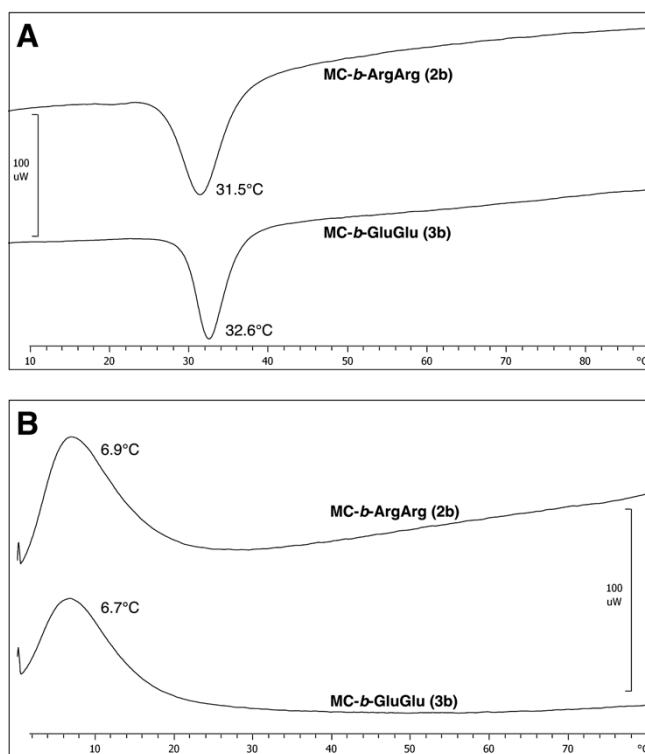


328 **Figure 7.** Hydrodynamic diameters of 0.2 wt% aqueous solutions of compounds **1b** (orange solid
 329 squares), **2b** (green solid triangles), **3b** (purple solid circles), and commercial MC (black solid
 330 diamonds) as functions of temperature.

331

332 Figure 8 shows the DSC thermograms of 2 wt% aqueous solutions of
 333 compounds **2b** and **3b**. Endothermic peaks appear at 31.5 °C and 32.6 °C for
 334 compounds **2b** and **3b**, respectively. The endothermic temperatures of compounds
 335 **2b** and **3b** are closely related to the supramolecular aggregation temperatures
 336 determined by DLS. The endothermic peaks observed by DSC are attributed to
 337 dehydration around the peptide-end-functionalized MCs **2b** and **3b**. Dehydration
 338 around these cellulosic molecules promotes their supramolecular aggregation, as
 339 shown in Figure 7.

340



341 **Figure 8.** DSC thermograms of 2.0 wt% aqueous solutions of compounds **2b** and **3b**: (A) heating
 342 curves (3.5 °C/min) and (B) cooling curves (3.5 °C/min).













343

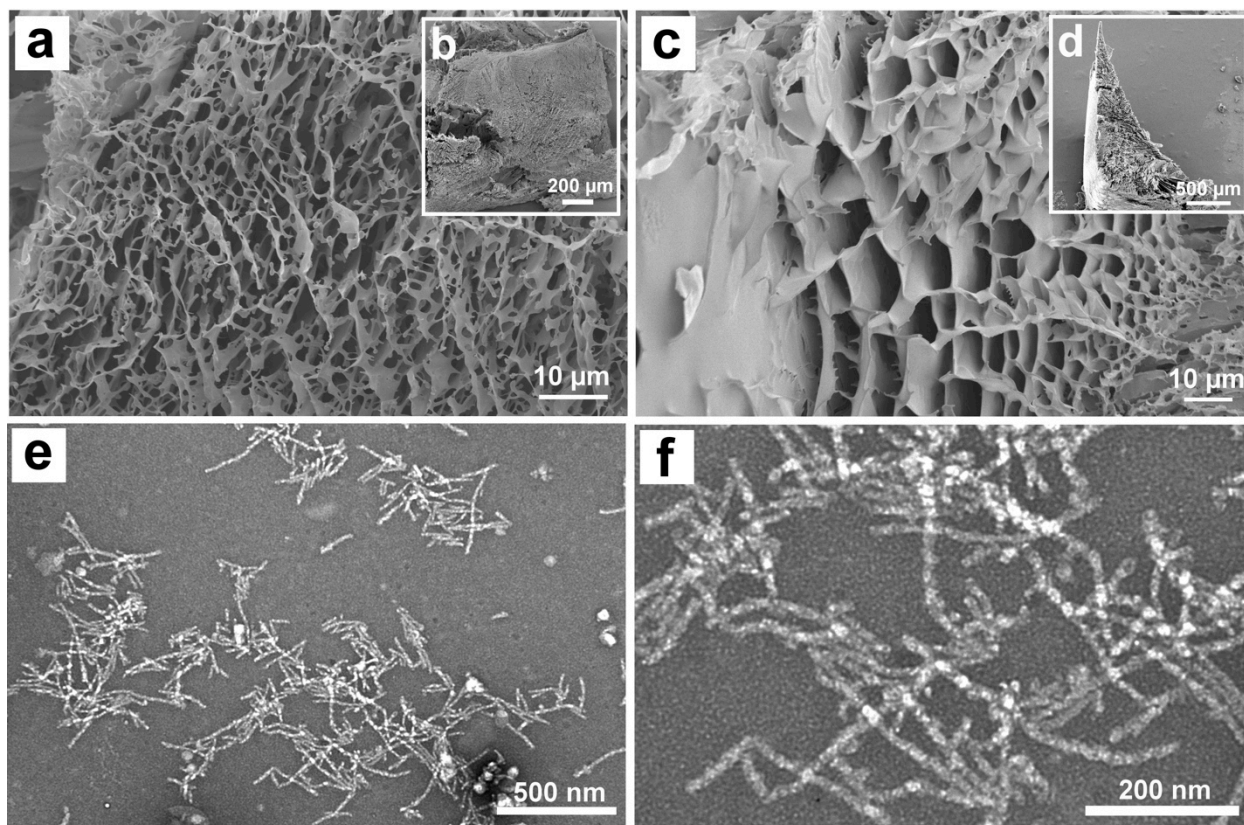
344 Table 2 displays images of 2.0 and 4.0 wt% aqueous solutions of compounds **1b**,
 345 **2b**, and **3b** at 0 and 35 °C. The 2 wt% aqueous solution of the cellobiose-
 346 functionalized MC **1b** forms a hydrogel at 35 °C. In contrast, the peptide-
 347 functionalized MCs **2b** and **3b** do not form hydrogels at 35 °C, rather their
 348 solutions became turbid at this temperature. In other words, the 2.0 wt% aqueous
 349 solutions of **2b** and **3b** phase separate at 35 °C. However, 4.0 wt% aqueous
 350 solutions of **1b**, **2b**, and **3b** form hydrogels at 35 °C. The concentrations of the
 351 thermally induced supramolecular structures of **2b** and **3b** are the keys to forming
 352 thermo-reversible hydrogels because 4.0 wt% aqueous solutions of the peptide-
 353 functionalized MCs **2b** and **3b** form hydrogels at 35 °C.

354

355

356 **Table 2.** Images of 2.0 and 4.0 wt% aqueous solutions of compounds **1b**, **2b**, and **3b**.

Comp. No.	Concentration: 2.0 wt %		Concentration: 4.0 wt %	
	Temperature (°C)		Temperature (°C)	
	0	35	0	35
1b				
2b				
3b				



357

358 **Figure 9.** SEM images of the hydrogels of (a, b) **2b** and (c, d) **3b**. (e, f) TEM images of the
 359 hydrogel of **2b**. Insets (b) and (d) are enlargements of regions in panels (a) and (c).

360

361 **Lyophilized hydrogels from compounds 2b and 3b**

362 SEM images of lyophilized hydrogels of **2b** and **3b** are shown in Figures 9a–d.
363 We previously reported that methylcellulose end-functionalized with cellobiose
364 exhibits a layered structure (Yamagami et al. 2018). In contrast, the peptide-
365 functionalized methylcelluloses **2b** and **3b** form a three-dimensional mesh
366 structure (**2b**) and a spongy, foam-like structure (**3b**), indicating that the
367 hydrophilic segments at the ends of the methylcellulose units of the lyophilized
368 hydrogels have different nanostructures.

369 **TEM images of the nanostructure of the thermoresponsive**
370 **supramolecular hydrogel of 2b**

371 TEM images of the hydrogel of compound **2b** are shown in Figures 9e–f, in
372 which regular stick-like structures with orthogonal widths of approximately 12 nm
373 and 15 nm, can be seen. The widths of the stick-like structures are constant,
374 although their lengths vary widely. The molecular length of compound **2b** is ~16
375 nm, which suggests that the longer width of a single rectangular structure is likely
376 to correspond to the molecular length of compound **2b**. The average thickness of
377 these structures was determined by atomic force microscopy to be approximately
378 10 nm (data not shown). Rectangular self-assemblies appear to form stick-like
379 structures, and their entanglements produce a macroscopic hydrogel.

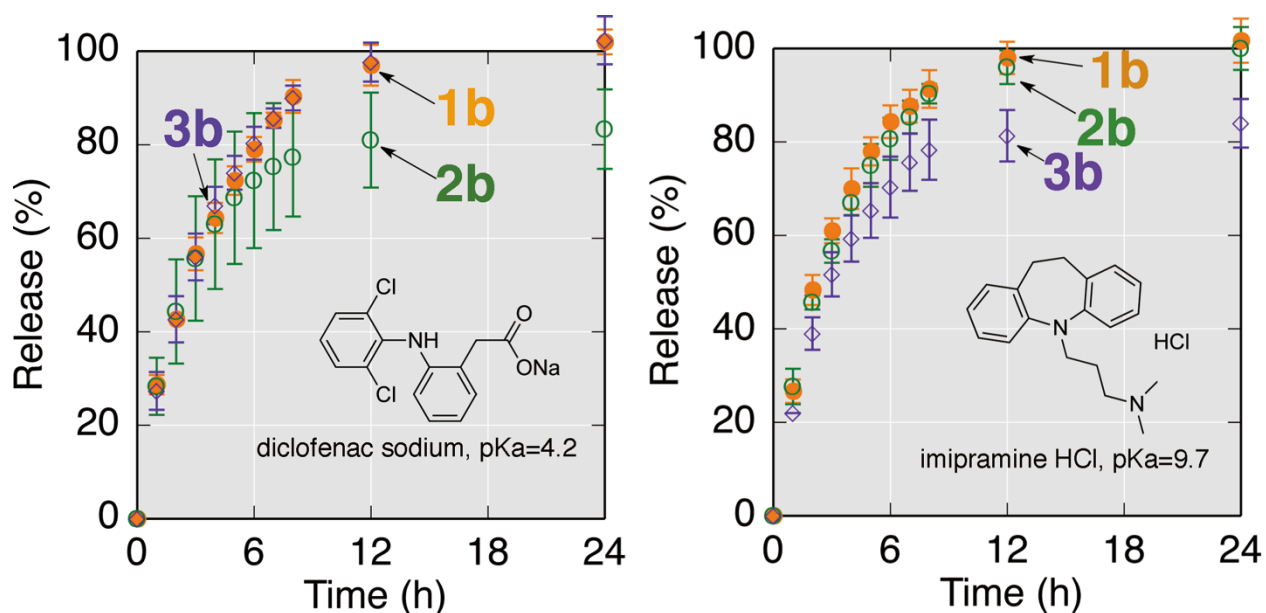
380 **Drug release from thermoresponsive supramolecular hydrogel**
381 **matrices**

382 The thermo-reversible supramolecular hydrogels of MCs **2b** and **3b** end-
383 functionalized with cationic and anionic peptides, respectively, are expected to
384 interact with anionic and cationic compounds, respectively. Therefore, we
385 investigated the ionic drug-release behavior of these hydrogels. To that end,

386 diclofenac sodium and imipramine were selected as model anionic and cationic
387 drugs, respectively.

388 Figure 10 displays the drug-release behavior of the thermoresponsive
389 supramolecular hydrogel matrices of **1b**, **2b**, and **3b**. These matrices exhibit
390 almost the same release behavior for diclofenac sodium (DFNa) at 37 °C at the
391 start of release testing. Approximately 28–29% of the DFNa was released from
392 hydrogel matrices **1b**, **2b**, and **3b** after 1 h. After 12 h, ~81% of the DFNa was
393 released from cationic hydrogel matrix **2b**, while ~100% of the DFNa was
394 released from the nonionic and anionic hydrogel matrices **1b** and **3b**. This
395 observation indicates that the cationic di(arginine) segment at the end of the MC
396 affects the release behavior of the anionic DFNa from the thermoresponsive
397 supramolecular hydrogel matrix.

398 In contrast, cationic imipramine interacts with anionic supramolecular hydrogel
399 matrix **3b**. At the beginning of imipramine-release testing (after 1 h of incubation)
400 27%, 28%, and 22% of the imipramine was released from hydrogel matrices **1b**,
401 **2b**, and **3b**, respectively. After 12 h, 98%, 96%, and 81% of the imipramine was
402 released from hydrogel matrices **1b**, **2b**, and **3b**, respectively, which indicates that
403 the anionic di(glutamic acid) segment at the end of the MC interacts with the
404 cationic imipramine. Ionic interactions between the cationic imipramine and the
405 anionic hydrogel matrix **3b** promote the relatively slow release of imipramine
406 from the thermoresponsive supramolecular hydrogel matrix.



407

408 **Figure 10.** Drug-release behavior from the thermoresponsive supramolecular hydrogel matrices of
 409 **1b** (orange solid circles), **2b** (green open circles), and **3b** (purple open diamonds).

410

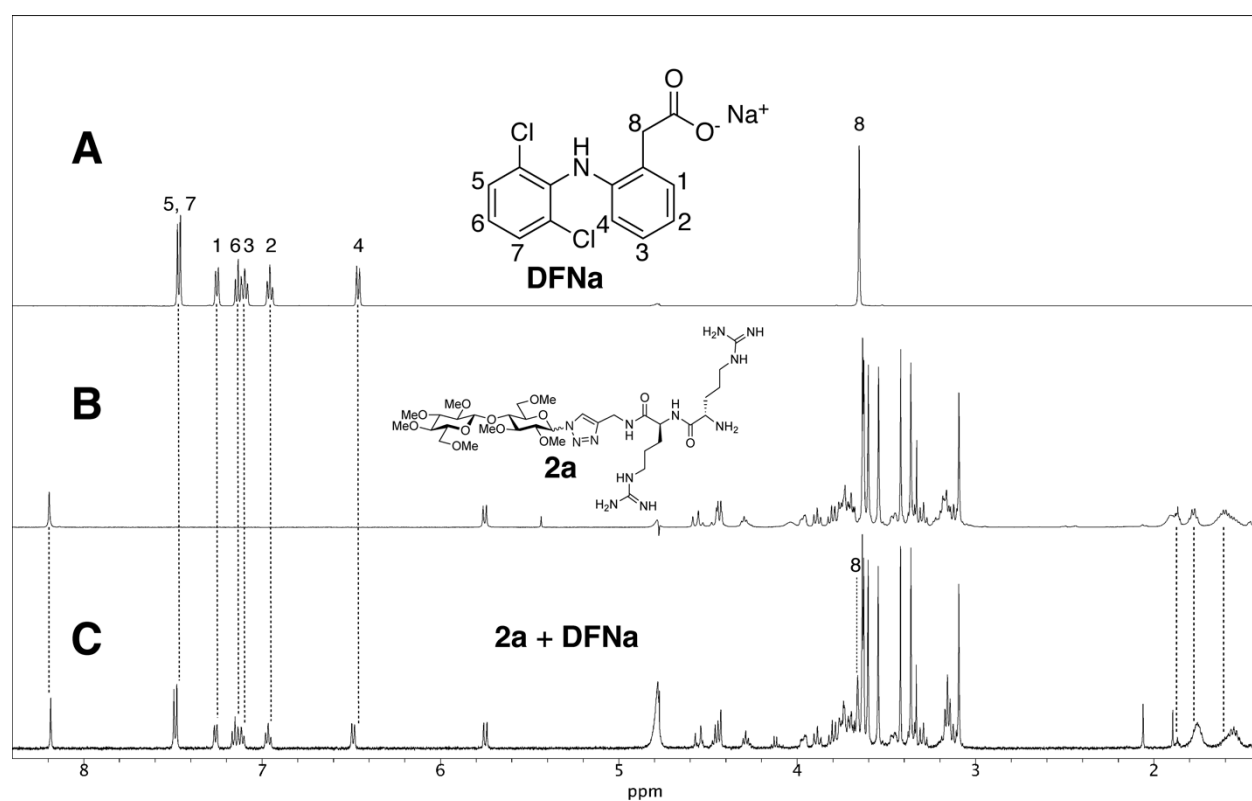
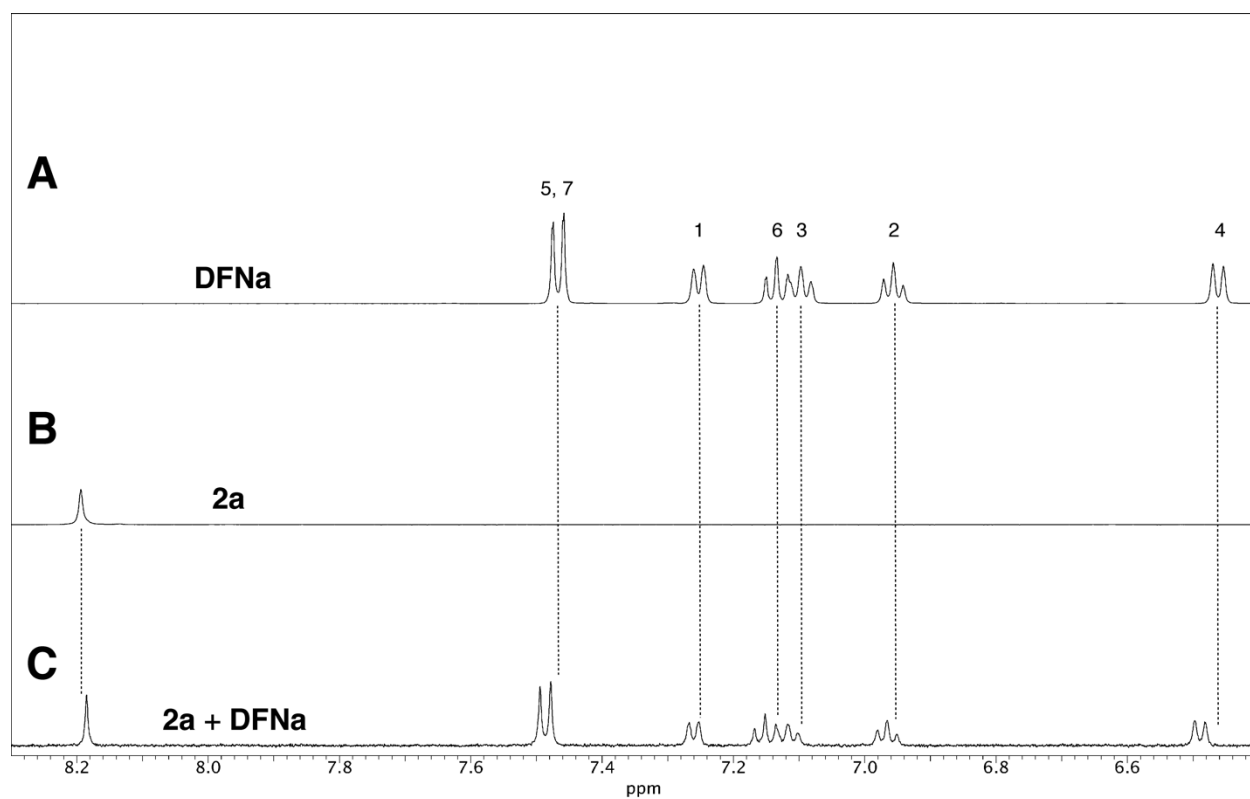
411 To gain deep insight into the interaction between the model drugs and the MCs
 412 end-functionalized with peptides, we performed $^1\text{H-NMR}$ experiments involving
 413 DFNa, methylated cellobiose derivative **2a** (a model compound of the MC end-
 414 functionalized with di(arginine) **2b**), and a mixture of DFNa and **2a**, in deuterium
 415 oxide.

416 Figure 11 reveals changes in the chemical shifts corresponding to both
 417 compounds, namely DFNa and **2a**, following mixing. After mixing anionic DFNa
 418 and cationic **2a** in D_2O , the proton resonances of DFNa, numbered 1 to 8, were
 419 observed to shift downfield by 0.007, 0.010, 0.020, 0.033, 0.019, 0.019, 0.019,
 420 and 0.009 ppm, respectively, which indicates that all of the protons in DFNa
 421 became deshielded through the removal of electron density. In contrast, the
 422 methylene protons of the arginine side-chain appear at higher magnetic fields
 423 following mixing, which indicate that these protons have become shielded due to
 424 an increase in electron density. In addition, the triazole proton of **2a**, which

425 resonated at 8.19 ppm prior to mixing, also appeared at slightly higher magnetic
426 field following mixing with DFNa.

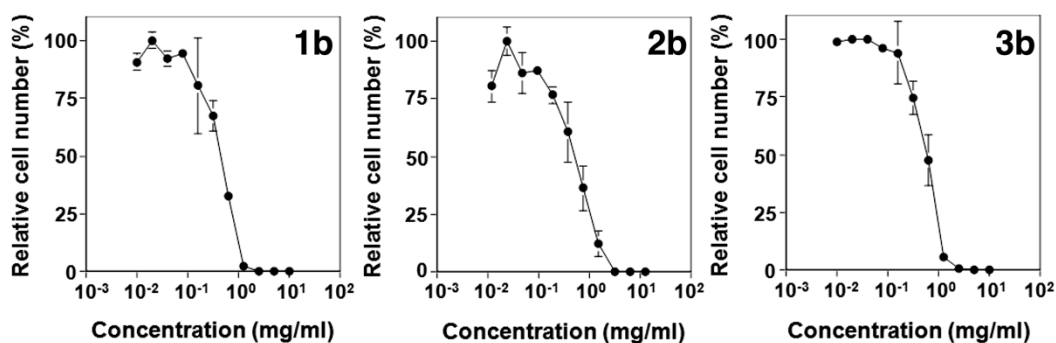
427 These observations indicate that supramolecular hydrogels of methylcellulose
428 end-functionalized with ionic peptides are expected to not only be
429 thermoresponsive but also pH responsive. This temperature/pH dual-
430 responsivenesses of compounds **2b** and **3b** are currently under investigation.

431



432 **Figure 11.** $^1\text{H-NMR}$ analyses of the interactions between compound **2b** and diclofenac sodium.

433



434 **Figure 12.** Inhibition of U937 cell growth by compounds **1b**, **2b**, and **3b**.

435

436 **Cytotoxicities of compounds 1b, 2b, and 3b**

437 ATP-based U937 histiocytoma cell-viability assays reveal that the half maximal
 438 inhibitory concentrations (IC_{50} values) of compounds **1b**, **2b**, and **3b** were 470,
 439 560, and 600 $\mu\text{g/mL}$, respectively, as shown in Figure 12. As previously noted, 4
 440 wt% aqueous solutions (40 mg/mL) of compounds **2b** and **2c** become
 441 supramolecular thermoresponsive hydrogels at 37 °C (see Table 2). The
 442 hydrogelation of an aqueous solution of compound **2b** or **2c** is likely to inhibit cell
 443 growth of suspension-type cells such as U937. However, the cytotoxicities of
 444 aqueous solutions of compounds **2b** and **2c**, determined by IC_{50} values, have been
 445 evaluated correctly, despite some supramolecular structures potentially present in
 446 the aqueous solutions. In summary, methylcelluloses end-functionalized with
 447 peptides are essentially nontoxic to U937 histiocytoma cells because IC_{50} values of
 448 0.6 wt% are considerably high.

449

450 **Conclusion**

451 Aqueous solutions of methylcelluloses end-functionalized with peptides exhibit
 452 supramolecular thermoresponsive hydrogelation behavior equivalent to those of
 453 block-functionalization methylcelluloses (Nakagawa et al. 2011a; Nakagawa et al.
 454 2012c; Yamagami et al. 2018). The tri-*O*-methylcellulose block, as a hydrophobic
 455 segment (Kamitakahara et al. 2016), is a key structure for supramolecular

456 thermoresponsive hydrogelation. Investigation into the relationships between the
457 anomeric configuration at the reducing-end of the tri-*O*-methylcellulose block and
458 physico-chemical properties in solution is now in progress. We were able to not
459 only introduce carbohydrates (Yamagami et al. 2018) but also peptides as
460 hydrophilic segments at the ends of hydrophobic tri-*O*-methylcellulose units,
461 resulting in the syntheses of a pool of diblock methylcellulose analogues with
462 biological functions that retain thermoresponsive hydrogelation behavior at
463 human-body temperature. As methylcellulose is produced from cellulose, which is
464 a natural resource, methylcelluloses end-functionalized with peptides are expected
465 to be used in biomedical applications as, for example, comparatively safe
466 injectable hydrogels.

467

468 **Experimental Section**

469 **Materials.**

470 *N*α-(9-Fluorenylmethoxycarbonyl)-*N*ω-(2,2,4,6,7-
471 pentamethyldihydrobenzofuran-5-sulfonyl)-L-arginine (*N*α-Fmoc-*N*ω-Pbf-L-
472 arginine) was purchased from Watanabe Chemical Industries, Ltd., Japan. *N*α-(9-
473 Fluorenylmethoxycarbonyl)glutamic acid γ -tert-butyl ester monohydrate (Fmoc-
474 Glu(*O**t*-Bu)-OH) was purchased from Peptide Institute, Inc., Japan. Other
475 chemicals were purchased from Nacalai Tesque, Wako Pure Chemicals, Tokyo
476 Chemical Industry, and Sigma-Aldrich. All reagents and solvents were of
477 commercial grade and were used without further purification.

478 **Synthesis.**

479 ***N*α-Fmoc-*N*ω-Pbf-L-arginine-*N*-propargylamide (12)**

480 *N*α-Fmoc-*N*ω-Pbf-L-arginine-*N*-propargylamide (**12**) (Yang et al. 2011) was
481 prepared from *N*α-Fmoc-*N*ω-Pbf-L-arginine (**11**) (89% yield). Briefly, to a
482 solution of *N*α-Fmoc-*N*ω-Pbf-L-arginine (**11**, 200 mg) in methanol (5 mL) was
483 added propargylamine (19 μL) and 4-(4,6-dimethoxy-1,3,5-triazin-2-yl)-4-
484 methylmorpholinium chloride (DMT-MM, 102 mg). The reaction mixture was
485 stirred for 3 h under nitrogen. The crude product was purified by preparative
486 silica-gel thin-layer chromatography (PTLC, eluent: 10% MeOH/CH₂Cl₂) to give
487 compound **12** (188 mg, 89% yield).

488 ¹H-NMR (500 MHz, CDCl₃): δ 1.42 (6H, CH₃, Pbf), 1.55-1.58 (m, 2H, H_γ),
489 1.85 (m, 2H, H_β), 2.07 (s, 3H, CH₃, Pbf), 2.14 (t, 1H, *J*=2.0 Hz, CH₂CCH), 2.50
490 (s, 3H, CH₃, Pbf), 2.57 (s, 3H, CH₃, Pbf), 2.91 (s, 2H, CH₂, Pbf), 3.28 (m, 2H, H_δ),
491 3.98 (m, 2H, CH₂CCH), 4.14 (t, 1H, *J*=7.0 Hz, CH, Fmoc), 4.27 (m, 1H, H_α),
492 4.34 (d, 2H, *J*=7.0 Hz, Fmoc), 7.24-7.74 (arom. Fmoc)

493 ¹³C-NMR (125 MHz, CDCl₃): δ 12.4 (CH₃, Pbf), 17.9 (CH₃, Pbf), 19.3 (CH₃,
494 Pbf), 25.2 (C_γ), 28.5 (CH₃, Pbf), 29.1 (CH₂CCH), 30.1 (C_β), 40.5 (C_δ), 43.1 (CH₂,
495 Pbf), 46.9 (CH, Fmoc), 54.1 (C_α), 67.1 (CH₂, Fmoc), 71.3 (CH₂CCH), 79.4
496 (CH₂CCH), 86.4 (C, Pbf), 117.5 (arom. Pbf), 119.9 (arom. Fmoc), 124.7 (arom.
497 Pbf), 125.1 (arom. Fmoc), 127.0 (arom. Fmoc), 127.7 (arom. Fmoc), 132.3 (arom.
498 Pbf), 138.4 (arom. Pbf), 141.1 (arom. Fmoc), 143.6 (arom. Fmoc), 143.7 (arom.
499 Fmoc), 156.3, 156.6 (CO Fmoc, quaternary C of guanidino group of arginine),
500 158.9 (-O-C arom. Pbf), 172.1 (Arg, C_α-CO-NH-)

501 ***N*ω-Pbf-L-arginine-*N*-propargylamide (**13**)**

502 *N*α-Fmoc-*N*ω-Pbf-L-arginine-*N*-propargylamide (**12**, 200 mg) was dissolved in
503 50% piperidine/dichloromethane (2 mL). The reaction mixture was stirred for 1 h
504 at room temperature under nitrogen, after which it was concentrated to dryness.

505 The crude product was extracted with ethyl acetate, washed with water and brine,
506 dried over sodium sulfate, and concentrated to dryness. The residue was purified
507 by silica-gel column chromatography (eluent: 15% methanol/dichloromethane,
508 v/v) to afford compound **13** (111 mg, 82% yield).

509 ¹H-NMR (500 MHz, CDCl₃): δ 1.47 (6H, CH₃, Pbf), 1.56-1.63 (m, 2H, H_γ),
510 1.80 (m, 2H, H_β), 2.09 (s, 3H, CH₃, Pbf), 2.22 (t, 1H, *J*=2.0 Hz, CH₂CCH), 2.50
511 (s, 3H, CH₃, Pbf), 2.57 (s, 3H, CH₃, Pbf), 2.96 (s, 2H, CH₂, Pbf), 3.22 (m, 2H, H_δ),
512 3.45 (t, 1H, H_α), 3.98 (m, 2H, CH₂CCH),

513 ¹³C-NMR (125 MHz, CDCl₃): δ 12.4 (CH₃, Pbf), 17.9 (CH₃, Pbf), 19.3 (CH₃,
514 Pbf), 25.4 (C_γ), 28.5 (CH₃, Pbf), 28.8 (CH₂CCH), 31.9 (C_β), 40.6 (C_δ), 43.2 (CH₂,
515 Pbf), 54.2 (C_α), 71.3 (CH₂CCH), 79.6 (CH₂CCH), 86.4 (C, Pbf), 117.5 (arom.
516 Pbf), 124.6 (arom. Pbf), 132.2 (arom. Pbf), 138.2 (arom. Pbf), 156.4 (quaternary
517 C of guanidino group of arginine), 158.9 (-O-C arom. Pbf), 175.1 (Arg, C_α-CO-
518 NH-)

519 ***N*α-Fmoc-*N*ω-Pbf-L-arginine-*N*ω-Pbf-L-arginine-*N*-propargylamide (9)**

520 (Morelli and Matile 2017)

521 To a solution of *N*α-Fmoc-*N*ω-Pbf-L-arginine (**11**, 101 mg, 1.2 equiv.) and *N*ω-
522 Pbf-L-arginine-*N*-propargylamide (**13**, 60 mg, 1.0 equiv.) in methanol (5 mL) was
523 added DMT-MM (43 mg, 1.2 equiv.). The reaction mixture was stirred for 4 h at
524 room temperature under nitrogen, and then concentrated to dryness. The crude
525 product was purified by PTLC (eluent: 10% methanol/dichloromethane) to afford
526 compound **9** as colorless crystals (126 mg, 89% yield).

527 ¹H-NMR (500 MHz, CDCl₃): δ 1.42 (12H, CH₃, Pbf), 1.63 (m, 4H, H_γ), 1.78
528 (m, 2H, H_β), 1.92 (m, 2H, H_β), 2.05 (s, 3H, CH₃, Pbf), 2.06 (s, 3H, CH₃, Pbf),
529 2.09 (1H, CH₂CCH), 2.48 (s, 3H, CH₃, Pbf), 2.49 (s, 3H, CH₃, Pbf), 2.55 (s, 3H,

530 CH₃, Pbf), 2.57 (s, 3H, CH₃, Pbf), 2.90 (s, 2H, CH₂, Pbf), 2.91 (s, 2H, CH₂, Pbf),
531 3.21 (m, 4H, H δ), 3.91-3.96 (m, 2H, CH₂CCH), 4.09 (t, 1H, *J*=7.0 Hz, CH, Fmoc),
532 4.27 (broad t, 1H, H α), 4.32-4.36 (d, d, 1H, 1H, *J*=7.0 Hz, Fmoc), 7.17-7.73
533 (arom. Fmoc)

534 ¹³C-NMR (125 MHz, CDCl₃): δ 12.4 (CH₃, Pbf), 17.9 (CH₃, Pbf), 19.3 (CH₃,
535 Pbf), 25.6 (C γ), 28.5 (CH₃, Pbf), 29.1 (CH₂CCH), 29.1 (C β), 40.0 (C δ), 40.6 (C δ),
536 43.1 (CH₂, Pbf), 46.9 (CH, Fmoc), 53.5 (C α), 55.1 (C α), 67.3 (CH₂, Fmoc), 71.3
537 (CH₂CCH), 79.4 (CH₂CCH), 86.4 (CH, Fmoc), 117.6 (arom. Pbf), 119.9 (arom.
538 Fmoc), 124.7 (arom. Pbf), 125.1 (arom. Fmoc), 127.0 (arom. Fmoc), 127.7 (arom.
539 Fmoc), 132.3 (arom. Pbf), 138.4 (arom. Pbf), 141.1 (arom. Fmoc), 143.7 (arom.
540 Fmoc), 156.4, 157.0 (CO Fmoc, quaternary C of guanidino group of arginine),
541 158.9 (-O-C arom. Pbf), 172.0 (Arg, C α -CO-NH-), 173.4 (Arg, C α -CO-NH-)

542 MALDI-TOF MS (*m/z*): calcd for C₅₆H₇₃N₉O₁₀S₂, 1095.49; found, [M+Na]⁺ =
543 1116.2

544 FT-IR (KBr): 3440, 3338, 2970, 2934, 1670, 1618, 1551, 1450, 1369, 1248, 1155,
545 1105, 853, 806, 783, 760, 741 (Fmoc), 669, 642, 621, 569 (Pbf, -SO₂NH-) cm⁻¹

546

547 **Fmoc-Glu(*Ot*-Bu)-*N*-propargylamide (15)** (Aagren et al. 2006)

548 To a solution of Fmoc-Glu(*Ot*-Bu)-OH (**14**, 300 mg) in methanol (5 mL) was
549 added propargylamine (52 μ L) and DMT-MM (102 mg). The reaction mixture
550 was stirred for 3 h under nitrogen. The crude product was purified by PTLC
551 (eluent: 10% MeOH/CH₂Cl₂) to give compound **15** as colorless crystals (324 mg,
552 quantitative yield).

553 $^1\text{H-NMR}$ (500 MHz, CDCl_3): δ 1.47 (s, 9H, CH_3 , *t*Bu), 1.96 (m, 1H, $\text{H}\beta$), 2.09
554 (m, 1H, $\text{H}\beta$), 2.22 (t, 1H, $J=2.0$ Hz, CH_2CCH), 2.33 (m, 1H, $\text{H}\gamma$), 2.43 (m, 1H,
555 $\text{H}\gamma$), 4.05 (broad s, 2H, CH_2CCH), 4.21 (2H, CH Fmoc, $\text{H}\alpha$), 4.41 (m, 2H, Fmoc),
556 5.78 (d, 1H, $J=7.5$ Hz, NH), 6.70 (broad s, 1H, NH), 7.32 (dt, 2H, $J=1.0$ Hz, $J=7.5$
557 Hz, Fmoc), 7.32 (dt, 2H, $J=1.0$ Hz, $J=1.0$ Hz, Fmoc), 7.41 (dt, 2H, $J=1.0$ Hz,
558 Fmoc), 7.77 (d, 2H, $J=7.5$ Hz, Fmoc),

559 $^{13}\text{C-NMR}$ (125 MHz, CDCl_3): δ 28.0 (CH_2CCH), 28.0 (CH_3 , *t*Bu), 39.2 ($\text{C}\beta$),
560 31.6 ($\text{C}\gamma$), 47.1 (CH , Fmoc), 54.1 ($\text{C}\alpha$), 67.1 (CH_2 , Fmoc), 71.8 (CH_2CCH), 79.1
561 (CH_2CCH), 81.2 (quaternary C of *t*Bu), 120.0 (arom. Fmoc), 125.0 (arom. Fmoc),
562 127.1 (arom. Fmoc), 127.7 (arom. Fmoc), 141.3 (arom. Fmoc), 143.7 (arom.
563 Fmoc), 156.3 (CO Fmoc), 171.0 (Glu, $-\text{C}\alpha-\text{CO}-\text{NH}-$), 173.0 (Glu, $\text{C}\delta\text{OO } t\text{Bu}$)

564 MALDI-TOF MS (m/z): calcd for $\text{C}_{27}\text{H}_{30}\text{N}_2\text{O}_5$, 462.22; found, $[\text{M}+\text{Na}]^+ = 485.2$,
565 $[\text{M}+\text{K}]^+ = 501.2$

566

567 **Glu(*O**t*-Bu)-*N*-propargylamide (16)** (Aagren et al. 2006)

568 Fmoc-Glu(*O**t*-Bu)-*N*-propargylamide (**15**, 308 mg) was dissolved in 50%
569 piperidine/dichloromethane (2 mL). The reaction mixture was stirred for 1 h at
570 room temperature under nitrogen, after which it was concentrated to dryness. The
571 crude product was extracted with ethyl acetate, washed with water and brine,
572 dried over sodium sulfate, and concentrated to dryness. The residue was purified
573 by silica-gel column chromatography (eluent: dichloromethane; eluent: 5%
574 methanol/dichloromethane, v/v) to afford compound **16** (166 mg, quantitative
575 yield).

576 $^1\text{H-NMR}$ (500 MHz, CDCl_3): δ 1.45 (s, 9H, CH_3 (*t*Bu)), 1.83 (m, 1H, $\text{H}\beta$), 2.09
577 (m, 1H, $\text{H}\beta$), 2.23 (t, 1H, $J=2.0$ Hz, CH_2CCH), 2.35 (m, 2H, $\text{H}\gamma$), 3.44 (t, 1H, $\text{H}\alpha$),
578 4.05 (broad s, 2H, CH_2CCH),

579 ^{13}C -NMR (125 MHz, CDCl_3): δ 28.0 (CH_3 (*t*Bu)), 28.8 (CH_2CCH), 30.1 ($\text{C}\beta$),
580 31.9 ($\text{C}\gamma$), 54.4 ($\text{C}\alpha$), 71.4 (CH_2CCH), 79.6 (CH_2CCH), 80.7 ($\text{C}(\text{CH}_3)_3$), 172.8
581 (Glu, $-\text{C}\alpha\text{-CO-NH-}$), 174.1 (Glu, $\text{C}\delta\text{OO } t\text{Bu}$)

582 MALDI-TOF MS (m/z): calcd for $\text{C}_{12}\text{H}_{20}\text{N}_2\text{O}_3$, 240.15; found, $[\text{M}+\text{Na}]^+ = 263.9$
583

584 ***N* α -Fmoc-Glu(*O**t*-Bu)-Glu(*O**t*-Bu)-*N*-propargylamide (10)**

585 To a solution of Fmoc-Glu(*O**t*-Bu)-OH (**14**, 328 mg, 1.2 equiv.) and Glu(*O**t*-
586 Bu)-*N*-propargylamide (**16**, 148 mg, 1.0 equiv.) in methanol (5 mL) was added
587 DMT-MM (204 mg, 1.2 equiv.). The reaction mixture was stirred for 1 h at room
588 temperature under nitrogen, and then concentrated to dryness. The crude product
589 was purified by PTLC (eluent: 5% methanol/dichloromethane) to afford
590 compound **10** as colorless crystals (378 mg, 95% yield).

591 ^1H -NMR (500 MHz, CDCl_3): δ 1.43 (s, 9H, CH_3 (*t*Bu)), 1.47 (s, 9H, CH_3 (*t*Bu)),
592 1.96-2.15 (m, 4H, $\text{H}\beta$), 2.13 (t, 1H, $J=2.0$ Hz, CH_2CCH), 2.33-2.47 (m, 4H, $\text{H}\gamma$),
593 3.96-4.03 (broad s, 2H, CH_2CCH), 4.20 (1H, H (Fmoc)), 4.20-4.24 (1H, $\text{H}\alpha$),
594 4.38-4.44 (m, 2H, CH_2 (Fmoc)), 4.48-4.49 (m, 1H, $\text{H}\alpha$), 7.30-7.77 (8H, arom.
595 Fmoc)

596 ^{13}C -NMR (125 MHz, CDCl_3): δ 27.0 ($\text{C}\beta'$), 27.4 ($\text{C}\beta$), 28.0 (CH_3 (*t*Bu)), 29.1
597 (CH_2CCH), 30.1 31.7 ($\text{C}\gamma'$), 31.8 ($\text{C}\gamma$), 52.6 ($\text{C}\alpha'$), 55.2 ($\text{C}\alpha$), 67.3 (CH_2 , Fmoc),
598 71.3 (CH_2CCH), 79.4 (CH_2CCH), 81.1 ($\text{C}(\text{CH}_3)_3$), 81.3 ($\text{C}(\text{CH}_3)_3$), 120.0, 125.1,
599 127.0, 127.7, 141.2, 143.7, 156.5, 170.6 (Glu, $-\text{C}\alpha\text{-CO-NH-}$), 171.6 (Glu, $-\text{C}\alpha\text{-$
600 CO-NH-), 173.0 (Glu, $\text{C}\delta\text{OO } t\text{Bu}$), 173.2 (Glu, $\text{C}\delta\text{OO } t\text{Bu}$)

601 MALDI-TOF MS (m/z): calcd for $\text{C}_{36}\text{H}_{45}\text{N}_3\text{O}_8$, 647.32; found, $[\text{M}+\text{Na}]^+ = 670.4$

602 FT-IR (KBr): 3290, 2978, 1728, 1694, 1639, 1537 (*t*Bu), 1450, 1368, 1258,
603 1157, 851, 758, 741 (Fmoc), 673 cm^{-1}

604

605 **2,3,4,6-Tetra-*O*-methyl- β -D-glucopyranosyl-(1 \rightarrow 4)-2,3,6-tri-*O*-methyl- β -D-**
606 **glucopyranosyl azide (7a)**

607 A 60% suspension of sodium hydride in mineral oil (1.97 g, 82.1 mmol, 14.0
608 equiv.) was added to a solution of β -D-glucopyranosyl-(1 \rightarrow 4)- β -D-glucopyranosyl
609 azide (Schamann and Schafer 2003; Ying and Gervay-Hague 2003) (1.29 g, 3.51
610 mmol) in DMF (30 mL) at 0 °C. The mixture was stirred at 0 °C for 1 h under
611 nitrogen. Methyl iodide (3.1 mL, 49.8 mmol, 14.2 equiv.) was then added to the
612 reaction mixture at 0 °C. After 2 h, the mixture was warmed to room temperature
613 and stirred for 2 h. The reaction was monitored by analytical thin-layer
614 chromatography (TLC). Methanol (0.43 mL) was added to deactivate the sodium
615 hydride. The mixture was concentrated and the crude product was extracted with
616 ethyl acetate, washed with distilled water, brine, dried over Na₂SO₄, and
617 concentrated to dryness. The residue was purified by silica-gel column
618 chromatography (eluent: 2:1 (v/v) ethyl acetate/*n*-hexane) to give colorless
619 crystals (**7a**, 0.799 g, 49% yield).

620 ¹H-NMR (500 MHz, CDCl₃): δ 2.86 (dd, 1H, $J=8.0$ Hz, $J=8.5$ Hz, H2'), 1H,
621 2.90 (t, 1H, $J=9.0$ Hz, H3'), 3.06 (t, 1H, $J=9.5$ Hz, H3'), 3.12 (t, 1H, $J=9.5$ Hz,
622 H4'), 3.16 (ddd, 1H, $J=2.0$ Hz, $J=4.0$ Hz, $J=9.5$ Hz, H5'), 3.19 (t, 1H, $J=9.0$ Hz,
623 H3), 3.32 (s, 3H, OCH₃), 3.34 (s, 3H, OCH₃), 3.36 (ddd, 1H, $J=2.0$ Hz, $J=4.0$ Hz,
624 $J=10.0$ Hz, H5), 3.46 (s, 3H, OCH₃), 3.48 (s, 3H, OCH₃), 3.52 (dd, 1H, $J=4.0$ Hz,
625 $J=11.0$ Hz, H6), 3.53 (s, 6H, OCH₃), 3.56 (s, 3H, OCH₃), 3.56 (dd, 1H, $J=2.0$ Hz,
626 $J=10.5$ Hz, H6'), 3.62 (dd, 1H, $J=9.0$ Hz, $J=10.0$ Hz, H4), 3.63 (dd, 1H, $J=2.0$ Hz,
627 $J=11.0$ Hz, H6), 3.67 (dd, 1H, $J=4.0$ Hz, $J=11.0$ Hz, H6), 4.23 (d, 1H, $J=7.5$ Hz,
628 H1'), 4.40 (d, 1H, $J=8.5$ Hz, H1)

629 ^{13}C -NMR (125 MHz, CDCl_3): δ 103.2 (C1'), 89.9 (C1), 86.9 (C3'), 84.9 (C3),
630 84.0 (C2'), 82.8 (C2), 79.3 (C4'), 77.2 (C4), 76.9 (C5), 74.7 (C5'), 71.2 (C6'), 70.1
631 (C6), 60.8, 60.6, 60.6, 60.6, 60.3, 59.3, 59.2 (OCH_3)

632

633 Tri-*O*-methylcellulosyl azide (**7b**) Compound **7b** was prepared according to our
634 previous paper (Kamitakahara et al. 2016).

635 FT-IR (KBr): 3478, 2926, 2836, 2116 (N_3), 1458, 1375, 1314, 1182, 1061, 949,
636 664 cm^{-1}

637

638 **2-Propynyl 2,3,6-tri-*O*-acetyl- β -D-glucopyranosyl-(1 \rightarrow 4)-2,3,6-tri-*O*-acetyl-**
639 **β -D-glucopyranoside (**8**)** Compound **8** was prepared according to our previous
640 paper (Yamagami et al. 2018).

641

642 **1-[2,3,4,6-Tetra-*O*-methyl- β -D-glucopyranosyl-(1 \rightarrow 4)-2,3,6-tri-*O*-methyl- β -**
643 **D-glucopyranosyl]-4-[2,3,4,6-tetra-*O*-acetyl- β -D-glucopyranosyl-(1 \rightarrow 4)-2,3,6-**
644 **tri-*O*-acetyl- β -D-glucopyranosyloxymethyl]-1*H*-1,2,3-triazole (**4a**)**

645 Azide **7a** (117 mg, 0.252 mmol) and glycoside **8** (170 mg, 0.252 mmol) were
646 dissolved in DMF (9 mL). Copper(I) bromide (361.5 mg, 2.52 mmol, 10 equiv.),
647 sodium ascorbate in water (998.5 mg/1.26 mL, 20 equiv.), and *N,N,N',N'',N''*-
648 pentamethyldiethylenetriamine (PMDETA, MW = 173.3, d = 0.83 g/mL, 0.5 mL,
649 10 equiv.) were added to the solution at room temperature. The reaction mixture
650 was stirred for 21 h. The insoluble component was then removed by filtration and
651 washed with dichloromethane. The washings and filtrate were combined and
652 concentrated, and the DMF was azeotropically removed with ethanol. The crude
653 product was purified by silica-gel column chromatography (eluent: 10%

654 MeOH/CH₂Cl₂) to give 1-[2,3,4,6-tetra-*O*-methyl-β-D-glucopyranosyl-(1→4)-
655 2,3,6-tri-*O*-methyl-β-D-glucopyranosyl]-4-[2,3,4,6-tetra-*O*-acetyl-β-D-
656 glucopyranosyl-(1→4)-2,3,6-tri-*O*-acetyl-β-D-glucopyranosyloxymethyl]-1*H*-
657 1,2,3-triazole (**4a**, 161.3 mg, 56% yield).

658 ¹H-NMR (500 MHz, CDCl₃): δ 1.97, 1.99, 2.01, 2.01, 2.04, 2.09, 2.15 (COCH₃),
659 2.95 (t, 1H, *J*=8.5 Hz, H2'_{Me}), 3.15 (t, 1H, *J*=9.0 Hz, H3'_{Me}), 3.19 (s, 3H, OCH₃),
660 3.21 (t, 1H, *J*=9.0 Hz, H4'_{Me}), 3.26 (ddd, 1H, *J*=2 Hz, *J*=3.5 Hz, *J*=9.5 Hz, H5'_{Me}),
661 3.33 (s, 3H, OCH₃), 3.43 (s, 3H, OCH₃), 3.44 (t, 1H, *J*=9.0 Hz, H3_{Me}), 3.55 (s, 3H,
662 OCH₃), 3.57 (s, 3H, OCH₃), 3.64 (s, 6H, OCH₃), 3.6-3.7 (H6'_{Me}, H2_{Me}, H5_{Me}, H5_{Ac},
663 H5'_{Ac}), 3.75 (dd, 1H, *J*=4.0 Hz, *J*=11.0 Hz, H6_{Me}), 3.79 (t, 1H, *J*=9.5 Hz, H4_{Ac}),
664 3.82 (dd, 1H, *J*=9.0 Hz, *J*=10.0 Hz, H4_{Me}), 4.05 (dd, 1H, *J*=2.5 Hz, *J*=12.5 Hz,
665 H6_{Ac}), 4.11 (dd, 1H, *J*=5.0 Hz, *J*=12.0 Hz, H6'_{Ac}), 4.34 (d, 1H, *J*=8.0 Hz, H1'_{Me}),
666 4.36 (dd, 1H, *J*=4.0 Hz, *J*=12.0 Hz, H6_{Ac}), 4.52 (d, 1H, *J*=8.0 Hz, H1'_{Ac}), 4.56 (dd,
667 1H, *J*=2.0 Hz, *J*=12.0 Hz, H6'_{Ac}), 4.62 (d, 1H, *J*=8.0 Hz, H1_{Ac}), 4.81 (d, 1H,
668 *J*=13.0 Hz, OCH₂-triazole), 4.92 (d, 1H, *J*=13.0 Hz, OCH₂-triazole), 4.9-4.95
669 (H2_{Ac}, H2'_{Ac}), 5.07 (t, 1H, *J*=9.5 Hz, H4'_{Ac}), 5.15 (t, 1H, *J*=9.0 Hz, H3_{Ac}), 5.15 (t,
670 1H, *J*=9.0 Hz, H3'_{Ac}), 5.47 (d, 1H, *J*=9.5 Hz, H1_{Me}), 7.69 (s, 1H, triazole)

671 ¹³C-NMR (125 MHz, CDCl₃): δ 20.5, 20.6, 20.6, 20.9 (COCH₃), 59.0 (OCH₃),
672 59.4 (OCH₃), 60.3 (OCH₃), 60.4 (OCH₃), 60.7 (OCH₃), 60.7 (OCH₃), 60.8
673 (OCH₃), 61.5(C6'_{Ac}), 61.7 (C6_{Ac}), 62.8 (OCH₂-triazole), 67.8 (C4'_{Ac}), 70.0 (C6_{Me}),
674 71.2 (C6'_{Me}), 71.4 (C2_{Ac} or C2'_{Ac}), 71.6 (C2_{Ac} or C2'_{Ac}), 72.0 (C5_{Ac}), 72.4 (C5'_{Ac}),
675 72.8 (C3_{Ac} or C3'_{Ac}), 72.9 (C3_{Ac} or C3'_{Ac}), 74.8 (C5'_{Me}), 76.3(C4_{Ac}), 77.9 (C4_{Me}),
676 79.3 (C4'_{Me}), 82.1 (C2_{Me}), 84.0 (C2'_{Me}), 85.2 (C3_{Me}), 87.0 (C3'_{Me}), 87.3 (C1_{Me}),
677 99.6 (C1_{Ac}), 100.7 (C1'_{Ac}), 103.3 (C1'_{Me}), 122.0 (triazole CH), 144.3 (O-CH₂-C=),
678 169.0, 169.3, 169.6, 169.7, 170.2, 170.5 (COCH₃)

679 **1-[2,3,4,6-Tetra-*O*-methyl- β -D-glucopyranosyl-(1 \rightarrow 4)-2,3,6-tri-*O*-methyl- β -**
680 **D-glucopyranosyl]-4-[β -D-glucopyranosyl-(1 \rightarrow 4)- β -D-**
681 **glucopyranosyloxymethyl]-1*H*-1,2,3-triazole (1a)**

682 Sodium methoxide (28%) in methanol (0.01 mL, 1.4 equiv.) was added at room
683 temperature to a solution of 1-[2,3,4,6-tetra-*O*-methyl- β -D-glucopyranosyl-
684 (1 \rightarrow 4)-2,3,6-tri-*O*-methyl- β -D-glucopyranosyl]-4-[2,3,4,6-tetra-*O*-acetyl- β -D-
685 glucopyranosyl-(1 \rightarrow 4)-2,3,6-tri-*O*-acetyl- β -D-glucopyranosyloxymethyl]-1*H*-
686 1,2,3-triazole (**4a**, 146 mg, 0.128 mmol) in MeOH (1 mL) and THF (1 mL). The
687 mixture was stirred for 3 h at room temperature. The solution was neutralized with
688 Amberlyst H⁺. The Amberlyst H⁺ was removed by filtration and washed with
689 MeOH. The combined filtrate and washings were concentrated to dryness to give
690 1-[2,3,4,6-tetra-*O*-methyl- β -D-glucopyranosyl-(1 \rightarrow 4)-2,3,6-tri-*O*-methyl- β -D-
691 glucopyranosyl]-4-[β -D-glucopyranosyl-(1 \rightarrow 4)- β -D-glucopyranosyloxymethyl]-
692 1*H*-1,2,3-triazole (**1a**, 108.3 mg, quantitative yield).

693 ¹H-NMR (500 MHz, D₂O): δ 3.01 (t, 1H, $J=9.5$ Hz, H2'_{Me}), 3.03 (s, 3H, OCH₃),
694 3.18 (t, 1H, $J=10.0$ Hz, H4'_{Me}), 3.21 (H2_{OH}), 3.21 (H2'_{OH}), 3.25 (t, 1H, $J=10.0$ Hz,
695 H3'_{Me}), 3.25 (s, 3H, OCH₃), 3.28 (H4'_{OH}), 3.31 (s, 3H, OCH₃), 3.33-3.38 (m, 1H,
696 H5_{OH}), 3.36 (t, 1H, $J=9.0$ Hz, H3'_{OH}), 3.38 (H5'_{Me}), 3.43 (s, 3H, OCH₃), 3.49 (s,
697 3H, OCH₃), 3.5 (H3_{OH}), 3.50-3.56 (H4_{OH}), 3.52 (s, 6H, OCH₃), 3.56-3.7 (H6_{Me} and
698 H6'_{Me}), 3.58-3.86 (H6_{OH} and H6'_{OH}), 3.62 (H3_{Me}), 3.73 (t, 1H, $J=9.0$ Hz, H2_{Me}),
699 3.79 (t, 1H, $J=10.0$ Hz, H4_{Me}), 3.86 (m, 1H, H5_{Me}), 4.33 (d, 1H, $J=8.0$ Hz, H1'_{Me}),
700 4.38 (d, 1H, $J=8.5$ Hz, H1'_{OH}), 4.46 (d, 1H, $J=7.5$ Hz, H1_{OH}), 4.81 (d, 1H, $J=13.0$
701 Hz, OCH₂-triazole), 4.90 (d, 1H, $J=13.0$ Hz, OCH₂-triazole), 5.68 (d, 1H, $J=9.0$
702 Hz, H1_{Me}), 8.24 (s, 1H, triazole CH)

703 ^{13}C -NMR (125 MHz, D_2O): δ 61.0 (OCH_3), 61.1 (OCH_3), 62.3 (OCH_3), 62.6
704 (OCH_3), 62.6 (C6_{OH} or $\text{C6}'_{\text{OH}}$), 62.7 (OCH_3), 63.2 (OCH_3), 63.2 (C6_{OH} or $\text{C6}'_{\text{OH}}$),
705 64.6 (OCH_2 -triazole), 72.1 ($\text{C4}'_{\text{OH}}$), 72.4 (C6_{Me} or $\text{C6}'_{\text{Me}}$), 73.1 (C6_{Me} or $\text{C6}'_{\text{Me}}$),
706 75.4 ($\text{C2}'_{\text{OH}}$), 75.8 (C2_{OH}), 76.1 ($\text{C3}'_{\text{OH}}$), 76.9 (C3_{OH}), 77.4 (C5_{OH}), 78.1 (C5_{OH} or
707 $\text{C5}'_{\text{Me}}$), 78.6 (C4_{Me}), 78.7 (C5_{OH} or $\text{C5}'_{\text{Me}}$), 79.3 (C5_{Me}), 81.1 (C4_{OH}), 81.4 ($\text{C4}'_{\text{Me}}$),
708 83.9 (C2_{Me}), 85.4 ($\text{C2}'_{\text{Me}}$), 86.0 (C3_{Me}), 87.6 ($\text{C3}'_{\text{Me}}$), 88.9 (C1_{Me}), 104.1 (C1_{OH}),
709 105.1 ($\text{C1}'_{\text{Me}}$), 105.2 ($\text{C1}'_{\text{OH}}$), 127.5 (triazole CH), 146.9 ($\text{O-CH}_2\text{-C=}$)

710 MALDI-TOF MS (m/z): calcd for $\text{C}_{34}\text{H}_{59}\text{N}_3\text{O}_{21}$, 845.36; found, $[\text{M}+\text{Na}]^+ =$
711 868.586, $[\text{M}+\text{K}]^+ = 884.580$

712

713 **1-(2,3,6-Tri-*O*-methyl-cellulosyl)-4-[2,3,4,6-tetra-*O*-acetyl- β -D-**
714 **glucopyranosyl-(1 \rightarrow 4)-2,3,6-tri-*O*-acetyl- β -D-glucopyranosyloxymethyl]-1*H*-**
715 **1,2,3-triazole (4b)**

716 Compound **4b** was prepared according to our previous paper (Yamagami et al.
717 2018). GPC analysis: $M_n = 7.4 \times 10^3$, $M_w / M_n = 1.4$, $DP_n = 34.8$.

718

719 **1-(2,3,6-Tri-*O*-methyl-cellulosyl)-4-[β -D-glucopyranosyl-(1 \rightarrow 4)- β -D-**
720 **glucopyranosyloxymethyl]-1*H*-1,2,3-triazole (1b)**

721 Compound **1b** was prepared according to our previous paper (Yamagami et al.
722 2018). GPC analysis: $M_n = 6.8 \times 10^3$, $M_w / M_n = 1.4$, $DP_n = 33$.

723

724 **1-[2,3,4,6-Tetra-*O*-methyl- β -D-glucopyranosyl-(1 \rightarrow 4)-2,3,6-tri-*O*-methyl- β -**
725 **D-glucopyranosyl]-4-(*N* α -Fmoc-*N* ω -Pbf-L-arginine-*N* ω -Pbf-L-arginine-*N*-**
726 **methyl)-1*H*-1,2,3-triazole (5a)**

727 To a solution of 2,3,4,6-tetra-*O*-methyl- β -D-glucopyranosyl-(1 \rightarrow 4)-2,3,6-tri-*O*-
728 methyl- β -D-glucopyranosyl azide (**7a**, 25 mg, 0.054 mmol) and Fmoc-Arg(Pbf)-
729 Arg(Pbf)-NH-CH₂CCH (**9**, 59 mg, 0.054 mmol) in 3 mL of
730 methanol/dichloromethane (1/4, v/v) were added CuBr (77 mg, 0.054 mmol, 10
731 equiv.) and aqueous sodium ascorbate (213 mg/269 μ L). The reaction mixture
732 was stirred under nitrogen at room temperature for 2 h. The mixture was purified
733 by preparative TLC (eluent: 1:9 (v/v) methanol/dichloromethane) to give 1-
734 [2,3,4,6-tetra-*O*-methyl- β -D-glucopyranosyl-(1 \rightarrow 4)-2,3,6-tri-*O*-methyl- β -D-
735 glucopyranosyl]-4-(*N* α -Fmoc-*N* ω -Pbf-L-arginine-*N* ω -Pbf-L-arginine-*N*-methyl)-
736 1*H*-1,2,3-triazole (**5a**, 71 mg, 0.045 mmol, 85% yield).

737 ¹H-NMR (500 MHz, CDCl₃): δ : 1.44 (CH₃, Pbf), 1.59 (H γ), 1.85 (H β), 2.06-
738 2.09 (CH₃, Pbf), 2.49-2.59 (CH₃, Pbf), 2.92 (CH₂, Pbf), 2.94 (CH₂, Pbf), 2.92 (t,
739 1H, *J*=9.0 Hz, H2'_{Me}), 3.11 (OCH₃), (3.12 (t, 1H, *J*=9.0 Hz, H3'_{Me}), 3.15 (t, 1H,
740 *J*=9.0 Hz, H4'_{Me}), 3.21-3.25 (m, 1H, H5'_{Me}), 3.22 (OCH₃), 3.26 (H δ), 3.40 (OCH₃),
741 3.35 (t, 1H, *J*=8.5 Hz, H3_{Me}), 3.38 (OCH₃), 3.52 (OCH₃), 3.53 (OCH₃), 3.59
742 (OCH₃), 3.62 (OCH₃), 3.5-3.7 (H6'_{Me}, H2_{Me}, H5_{Me}), 3.6-3.75 (2H, H6_{Me}), 3.75 (t,
743 1H, *J*=9.5 Hz, H4_{Me}), 4.1-4.35 (broad s, H α), 4.18-4.24 (1H, H (Fmoc)), 4.30
744 (H1'_{Me}), 4.32-4.36 (CH₂, Fmoc), 4.43-4.60 (broad d, broad d, 2H, NH-CH₂-
745 triazole), 5.41 (H1_{Me}), 5.60 (NH), 6.0-6.6 (NH), 7.2-7.8 (arom. H, Fmoc)

746 ¹³C-NMR (125 MHz, CDCl₃): δ 12.5 (CH₃, Pbf), 17.9 (CH₃, Pbf), 19.3 (CH₃,
747 Pbf), 25.6 (C γ), 28.6 (CH₃, Pbf), 29.7 (C β), 40.8 (C δ), 43.2 (CH₂, Pbf), 47.0 (CH,
748 Fmoc), 53.6 (C α), 54.4 (C α), 58.7, 59.3, 60.4, 60.6, 60.8 (OCH₃), 67.3 (CH₂,
749 Fmoc), 70.1 (C6), 71.2 (C6'), 74.7 (C5'), 77.2 (C4), 77.4 (C5), 79.3 (C4'), 81.8
750 (C2), 84.0 (C2'), 85.2 (C3), 86.4 (CH, Fmoc), 86.4 (CH, Fmoc), 86.9 (C3'), 87.0
751 (C1), 103.3 (C1'), 117.6 (arom. Pbf), 119.9 (arom. Fmoc), 120.0, 122.5 (triazole

752 CH), 124.6 (arom. Pbf), 124.9 (arom. Fmoc), 125.2 (arom. Fmoc), 127.1 (arom.
753 Fmoc), 127.6 (arom. Fmoc), 132.3 (arom. Pbf), 132.7 (arom. Pbf), 138.3 (arom.
754 Pbf), 141.1 (arom. Fmoc), 143.7 (arom. Fmoc), 144.5 (O-CH₂-C=), 156.4 (arom.
755 Pbf), 158.7 (-O-C arom. Pbf), 172.2 (Arg, C α -CO-NH-), 173.5 (Arg, C α -CO-NH)
756 MALDI-TOF MS (*m/z*): calcd for C₇₅H₁₀₈N₁₂O₂₀S₂, 1560.72; found, [M+H]⁺ =
757 1559.755, [M+Na]⁺ = 1581.722, [M+K]⁺ = 1597.671

758

759 **1-[2,3,4,6-Tetra-*O*-methyl- β -D-glucopyranosyl-(1 \rightarrow 4)-2,3,6-tri-*O*-methyl- β -**
760 **D-glucopyranosyl]-4-(Arg-Arg-NH-CH₂)-1*H*-1,2,3-triazole (2a)**

761 1-[2,3,4,6-Tetra-*O*-methyl- β -D-glucopyranosyl-(1 \rightarrow 4)-2,3,6-tri-*O*-methyl- β -D-
762 glucopyranosyl]-4-(*N* α -Fmoc-*N* ω -Pbf-L-arginine-*N* ω -Pbf-L-arginine-*N*-methyl)-
763 1*H*-1,2,3-triazole (**5a**, 61 mg, 0.039 mmol) was dissolved in
764 piperidine/dichloromethane (1/1, v/v, 1 mL). The reaction mixture was stirred
765 under nitrogen at room temperature for 1 h and then concentrated to dryness. The
766 crude product was purified by preparative TLC (eluent: 15:85 (v/v)
767 methanol/dichloromethane) to give 1-[2,3,4,6-tetra-*O*-methyl- β -D-
768 glucopyranosyl-(1 \rightarrow 4)-2,3,6-tri-*O*-methyl- β -D-glucopyranosyl]-4-(*N* ω -Pbf-L-
769 arginine-*N* ω -Pbf-L-arginine-*N*-methyl)-1*H*-1,2,3-triazole (34 mg, 0.025 mmol,
770 65% yield; MALDI-TOF MS (*m/z*): calcd for C₆₀H₉₆N₁₂O₁₈S₂, 1336.64; found,
771 [M+Na]⁺ = 1359.5).

772 1-[2,3,4,6-Tetra-*O*-methyl- β -D-glucopyranosyl-(1 \rightarrow 4)-2,3,6-tri-*O*-methyl- β -D-
773 glucopyranosyl]-4-(*N* ω -Pbf-L-arginine-*N* ω -Pbf-L-arginine-*N*-methyl)-1*H*-1,2,3-
774 triazole (31 mg, 0.023 mmol) was dissolved in TFA/distilled water (8/2, v/v, 1.0
775 mL) and stirred under nitrogen at 37 °C for 4 h. The reaction mixture was
776 concentrated to dryness and the crude product was purified by gel-filtration

777 column chromatography (LH-20, eluent: methanol) to give 1-[2,3,4,6-tetra-*O*-
778 methyl- β -D-glucopyranosyl-(1 \rightarrow 4)-2,3,6-tri-*O*-methyl- β -D-glucopyranosyl]-4-
779 (Arg-Arg-NH-CH₂)-1*H*-1,2,3-triazole (**2a**, 10 mg, 0.012 mmol, 52% yield).

780 ¹H-NMR (500 MHz, D₂O): δ 1.5-1.7 (m, 4H, H γ and H γ'), 1.73-1.83 (m, 2H,
781 H β), 1.85-1.95 (m, 2H, H β'), 3.09 (s, 3H, OCH₃), 3.12 (t, *J*=9.5 Hz, H2'), 3.12-
782 3.25 (m, 4H, H δ and H δ'), 3.29 (t, *J*=9.0 Hz, H4'), 3.36 (t, *J*=9.0 Hz, H3'), 1H,
783 3.36 (s, 3H, OCH₃), 3.42 (s, 3H, OCH₃), 3.46 (m, 1H, H5'), 3.54 (s, 3H, OCH₃),
784 3.60 (s, 3H, OCH₃), 3.63 (s, 3H, OCH₃), 3.63 (s, 3H, OCH₃), 3.67-3.75 (2H, H6'),
785 3.70 (t, 1H, *J*=9.5 Hz, H3), 3.72-3.78 (2H, H6), 3.81 (t, 1H, *J*=9.0 Hz, H2), 3.89 (t,
786 1H, *J*=9.0 Hz, H4), 3.97 (m, 1H, H5), 4.04 (broad s, 1H, H α'), 4.30 (t, 1H, *J*=6.5
787 Hz, H α (near sugar residue)), 4.44 (d, 1H, *J*=8.0 Hz, H1'), 4.44 (d, 1H, *J*=14.5 Hz,
788 NHCH₂-triazole), 4.57 (d, 1H, *J*=15.5 Hz, OCH₂-triazole), 5.75 (d, 1H, *J*=9.5 Hz,
789 H1), 8.19 (s, 1H, CH, triazole)

790 ¹³C-NMR (125 MHz, D₂O): δ 26.0 (C γ'), 26.9 (C γ), 30.6 (C β or C β'), 30.8 (C β
791 or C β'), 36.8 (NHCH₂-triazole), 43.0 (C δ or C δ'), 43.1 (C δ or C δ'), 51.5 (C α'),
792 56.6 (C α (near sugar residue)), 61.0 (OCH₃), 61.1 (OCH₃), 62.4 (OCH₃), 62.5
793 (OCH₃), 62.6 (OCH₃), 62.7 (OCH₃), 63.2 (OCH₃), 72.5 (C6), 73.1 (C6'), 76.1
794 (C5'), 78.7 (C4), 79.3 (C5), 81.4 (C4'), 84.0 (C2), 85.4 (C2'), 86.0 (C3), 87.8 (C3'),
795 88.9 (C1), 105.1 (C1'), 126.2 (CH of triazole), 147.5 (quaternary C of triazole).
796 159.4 (quaternary C of guanidino group of arginine), 159.4 (quaternary C of
797 guanidino group of arginine), 175.8 (C α -CO-NH-), 175.9 (C α' -CO-NH-)

798 MALDI-TOF MS (*m/z*): calcd for C₃₄H₆₄N₁₂O₁₂, 832.48; found, [M+H]⁺ =
799 833.63

800

801 **1-[2,3,4,6-Tetra-*O*-methyl- β -D-glucopyranosyl-(1 \rightarrow 4)-2,3,6-tri-*O*-methyl- β -**
802 **D-glucopyranosyl]-4-[Fmoc-Glu(*O**t*-Bu)-Glu(*O**t*-Bu)-*N*-methyl]-1*H*-1,2,3-**
803 **triazole (6a)**

804 To a solution of 2,3,4,6-tetra-*O*-methyl- β -D-glucopyranosyl-(1 \rightarrow 4)-2,3,6-tri-*O*-
805 methyl- β -D-glucopyranosyl azide (**7a**, 25 mg, 0.054 mmol) and Fmoc-
806 Glu(*O**t*Bu)-Glu(*O**t*Bu)-NH-CH₂CCH (**10**, 35 mg, 0.054 mmol) in 3 mL of
807 methanol/dichloromethane (1/4, v/v) were added CuBr (77 mg, 0.054 mmol, 10
808 equiv.) and aqueous sodium ascorbate (213 mg/269 μ L). The reaction mixture
809 was stirred under nitrogen at room temperature for 2 h, after which it was purified
810 by PTLC (eluent: 1:9 (v/v) methanol/dichloromethane) to give 1-(2,3,4,6-tetra-*O*-
811 methyl- β -D-glucopyranosyl-(1 \rightarrow 4)-2,3,6-tri-*O*-methyl- β -D-glucopyranosyl)-4-
812 [*N* α -Fmoc-Glu(*O**t*-Bu)-Glu(*O**t*-Bu)-*N*-methyl]-1*H*-1,2,3-triazole (52 mg, 0.047
813 mmol, 87% yield).

814 ¹H-NMR (500 MHz, CDCl₃): δ : 1.42 (s, 9H, CH₃ (*t*Bu)), 1.46 (s, 9H, CH₃ (*t*Bu)),
815 1.90-2.02 (m, 2H, H β), 2.02-2.20 (m, 2H, H β), 2.26-2.48 (m, 4H, H γ), 2.96 (t, 1H,
816 $J=8.5$ Hz, H2'_{Me}), 3.14 (t, 1H, $J=9.0$ Hz, H3'_{Me}), 3.15 (s, 3H, OCH₃), 3.20 (t, 1H,
817 $J=8.5$ Hz, H4'_{Me}), 3.23-3.28 (H5'_{Me}), 3.30 (s, 3H, OCH₃), 3.39 (t, 1H, $J=8.5$ Hz,
818 H3_{Me}), 3.42 (s, 3H, OCH₃), 3.54 (s, 3H, OCH₃), 3.56 (s, 3H, OCH₃), 3.62 (s, 3H,
819 OCH₃), 3.63 (s, 3H, OCH₃), 3.54-3.58 (m, H5_{Me}), 3.58-3.67 (3H, H6_{Me}, H6'_{Me}),
820 3.64 (t, 1H, $J=9.0$ Hz, H2_{Me}), 3.6-3.75 (dd, 1H, $J=4.5$ Hz, $J=11.0$ Hz, H6_{Me}), 3.79
821 (t, 1H, $J=9.5$ Hz, H4_{Me}), 4.12 (m, 1H, H α), 4.20 (t, 1H, $J=4.5$ Hz, CH (Fmoc)),
822 4.32 (d, 1H, $J=8.0$ Hz, H1_{Me}), 4.35 (broad d, 2H, $J=7.0$ Hz, CH₂ (Fmoc)), 4.43 (m,
823 1H, H α), 4.54 (broad d, $J=5.5$ Hz, NH-CH₂-triazole), 5.39 (d, 1H, $J=9.0$ Hz, H1_{Me}),
824 6.07 (d, $J=6.0$ Hz, NH-C α), 7.28-7.78 (8H, arom. Fmoc), 7.74 (broad s, triazole
825 H)

826 ¹³C-NMR (125 MHz, CDCl₃): δ 27.0 (triazole-CH₂-NH-C_α-C_β-), 27.3 (C_β-C_α-
827 NH-Fmoc), 28.0 (CH₃ (tBu)), 28.0 (CH₃ (tBu)), 31.8 (triazole-CH₂-NH-C_α-C_β-
828 C_γ), 31.8 (C_γ-C_β-C_α-NH-Fmoc), 35.1 (triazole-CH₂-NH-), 47.1 (CH, Fmoc),
829 53.0 (triazole-CH₂-NH-CO-C_α-NH-), 55.3 (-CO-C_α-NH-Fmoc), 59.0 (OCH₃),
830 59.3 (OCH₃), 60.3 (OCH₃), 60.3 (OCH₃), 60.6 (OCH₃), 60.7 (OCH₃), 60.8 (OCH₃),
831 67.1 (CH₂, Fmoc), 70.0 (C6), 71.1 (C6'), 74.7 (C5'), 77.1 (C4), 77.8 (C5), 79.3
832 (C4'), 81.1 (C(CH₃)₃), 81.3 (C(CH₃)₃), 81.9 (C2), 84.0 (C2'), 85.3 (C3), 86.9 (C3'),
833 87.2 (C1), 103.2 (C1'), 119.9 (arom. Fmoc), 121.6 (triazole CH), 125.2 (arom.
834 Fmoc), 127.1 (arom. Fmoc), 127.1 (arom. Fmoc), 127.7 (arom. Fmoc), 141.2
835 (arom. Fmoc), 141.3 (arom. Fmoc), 143.7 (arom. Fmoc), 143.9 (arom. Fmoc),
836 144.8 (O-CH₂-C=), 156.6 (CO Fmoc), 171.0 (Glu, triazole-CH₂-NH-CO-C_α-NH-),
837 171.6 (Glu, -CO-C_α-NH-Fmoc), 173.1 (Glu, Cδ), 173.1 (Glu, Cδ)

838 MALDI-TOF MS (*m/z*): calcd for C₅₅H₈₀N₆O₁₈, 1112.55; found, [M+Na]⁺ =
839 1135.615, [M+K]⁺ = 1151.583

840

841 **1-[2,3,4,6-Tetra-*O*-methyl-β-D-glucopyranosyl-(1→4)-2,3,6-tri-*O*-methyl-β-**
842 **D-glucopyranosyl]-4-(Glu-Glu-NH-CH₂)-1*H*-1,2,3-triazole (3a)**

843 1-[2,3,4,6-Tetra-*O*-methyl-β-D-glucopyranosyl-(1→4)-2,3,6-tri-*O*-methyl-β-D-
844 glucopyranosyl]-4-[*N*α-Fmoc-Glu(*O**t*-Bu)-Glu(*O**t*-Bu)-*N*-methyl]-1*H*-1,2,3-
845 triazole (**6a**, 46 mg, 0.034 mmol) was dissolved in piperidine/dichloromethane
846 (1/1, v/v, 1 mL). The reaction mixture was stirred under nitrogen at room
847 temperature for 1 h, and then concentrated to dryness. The crude product was
848 purified by PTLC (eluent: methanol/dichloromethane (15/85, v/v)) to give 1-
849 [2,3,4,6-tetra-*O*-methyl-β-D-glucopyranosyl-(1→4)-2,3,6-tri-*O*-methyl-β-D-

850 glucopyranosyl]-4-[Glu(*Ot*-Bu)-Glu(*Ot*-Bu)-*N*-methyl]-1*H*-1,2,3-triazole (24 mg,
851 0.016 mmol, 47% yield).

852 1-[2,3,4,6-Tetra-*O*-methyl- β -D-glucopyranosyl-(1 \rightarrow 4)-2,3,6-tri-*O*-methyl- β -D-
853 glucopyranosyl]-4-(Glu(*Ot*-Bu)-Glu(*Ot*-Bu)-*N*-methyl)-1*H*-1,2,3-triazole (66 mg,
854 0.079 mmol) was dissolved in TFA/dichloromethane (9/1, v/v, 1 mL) and stirred
855 under nitrogen at room temperature for 4 h. The crude product was purified by
856 gel-filtration chromatography (LH-20, eluent: methanol) to give 1-[2,3,4,6-tetra-
857 *O*-methyl- β -D-glucopyranosyl-(1 \rightarrow 4)-2,3,6-tri-*O*-methyl- β -D-glucopyranosyl]-4-
858 (Glu-Glu-*N*-methyl)-1*H*-1,2,3-triazole (**3a**, 36 mg, 0.046 mmol, 58% yield).

859 ¹H-NMR (500 MHz, D₂O): δ 1.9-2.1 (m, 2H, H β), 2.2-2.3 (m, 2H, H β), 2.3-2.6
860 (m, 4H, H γ), 3.12 (t, 1H, $J=8.5$ Hz, H2'_{Me}), 3.29 (t, 1H, $J=9.5$ Hz, H4'_{Me}), 3.36 (t,
861 1H, $J=8.5$ Hz, H3'_{Me}), 3.36 (s, 3H, OCH₃), 3.42 (s, 3H, OCH₃), 3.43-3.48 (H5'_{Me}),
862 3.54 (s, 3H, OCH₃), 3.60 (s, 3H, OCH₃), 3.62 (s, 3H, OCH₃), 3.63 (s, 6H, OCH₃),
863 3.7 (H3_{Me}), 3.80 (t, 1H, $J=9.5$ Hz, H2_{Me}), 3.89 (t, 1H, $J=9.5$ Hz, H4_{Me}), 3.93-3.98
864 (m, 1H, H5_{Me}), 3.65-3.83 (H6'_{Me}, H6_{Me}), 3.79 (t, 1H, $J=9.5$ Hz, H4_{Me}), 3.86 (m, 1H,
865 H5_{Me}), 4.2-4.5 (broad s, 1H, H α), 4.34 (d, 1H, $J=8.0$ Hz, H1'_{Me}), 4.4-4.61 (NH-
866 CH₂-triazole), 5.75 (broad d, 1H, $J=7.0$ Hz, H1_{Me}), 8.24 (broad s, triazole *CH*)

867 ¹³C-NMR (125 MHz, D₂O): δ 27.9 (C β '), 29.0 (C β), 31.9 (C γ and C γ '), 37.1
868 (NHCH₂-triazole), 56.1 (C α (near sugar residue)), 59.4 (C α '), 61.1 (OCH₃), 61.2
869 (OCH₃), 62.2 (OCH₃), 62.5 (OCH₃), 62.6 (OCH₃), 62.7 (OCH₃), 63.2 (OCH₃),
870 72.5 (C6 or C6'), 73.1 (C6 or C6'), 76.1 (C5'), 78.7 (C4), 79.4 (C5), 81.5 (C4'),
871 84.0 (C2), 85.5 (C2'), 86.0 (C3), 87.8 (C3'), 89.1 (C1), 105.2 (C1'), 126.6 (CH of
872 triazole), 177.6 (C α -CO-NH-, and C α '-CO-NH-), 184.9 (C γ -CO)OH, C γ '-
873 (CO)OH)

874 MALDI-TOF MS (m/z): calcd for $C_{32}H_{54}N_6O_{16}$, 778.36; found, $[M+H]^+ =$
875 779.518, $[M+Na]^+ = 801.530$, $[M+K]^+ = 817.504$

876

877 **1-(Tri-*O*-methylcellulosyl)-4-(*N* α -Fmoc-*N* ω -Pbf-L-arginine-*N* ω -Pbf-L-**
878 **arginine-*N*-methyl)-1*H*-1,2,3-triazole (**5b**)**

879 Sodium ascorbate (227 mg/287 μ L, 1.15 mmol, 20 equiv., 4 M in H_2O) and
880 $CuSO_4 \cdot 5H_2O$ (143 mg, MW = 249.69, 0.573 mmol, 10 equiv.) were added to a
881 solution of 2-propynyl *N* α -Fmoc-*N* ω -Pbf-L-arginine-*N* ω -Pbf-L-arginine-*N*-
882 propargylamide (**9**, 100 mg, MW = 788.8, 0.127 mmol, 2.2 equiv.) and tri-*O*-
883 methylcellulosyl azide (**7b**, 419 mg, $M_n = 7.34 \times 10^3$, $DP_n = 35.8$, 0.0571 mmol,
884 1.0 equiv.) in methanol/dichloromethane (1/4, v/v, 10 mL). The reaction mixture
885 was stirred at room temperature for 14 h under nitrogen, after which it was
886 concentrated and passed through a silica-gel chromatography column (eluent:
887 20% MeOH/ CH_2Cl_2) to give the crude product. The crude product was purified by
888 gel-filtration column chromatography (LH-60, eluent: 20% MeOH/ CH_2Cl_2) to
889 give 1-(tri-*O*-methylcellulosyl)-4-(*N* α -Fmoc-*N* ω -Pbf-L-arginine-*N* ω -Pbf-L-
890 arginine-*N*-methyl)-1*H*-1,2,3-triazole (**5b**, 420 mg, quantitative yield; GPC
891 analysis: $M_n = 5.6 \times 10^3$, $M_w / M_n = 1.8$).

892 1H -NMR (500 MHz, $CDCl_3$): δ : 1.44 (CH_3 , Pbf), 2.07 (CH_3 , Pbf), 2.47-2.56
893 (CH_3 , Pbf), 2.92 (CH_2 , Pbf), 2.96 (t, $J=8.5$ Hz, H_{2Me} (internal)), 3.21 (t, 1H, $J=9.0$
894 Hz, H_{3Me} (internal)), 3.29 (m, $J=9.0$ Hz, H_{5Me} (internal)), 3.39 (s, OCH_3), 3.54 (s,
895 OCH_3), 3.58 (s, OCH_3), 3.69 (t, $J=9.0$, H_{4Me} (internal)), 3.6-3.73 (m, H_{6Me}
896 (internal)), 3.77 (m, H_{6Me} (internal)), 4.34 (d, $J=8.0$ Hz, H_{1Me} (internal)), 6.12
897 ($H_{1\alpha Me}$), 6.1-6.7, 7.24 (Fmoc), 7.35 (Fmoc), 7.57 (Fmoc), 7.62 (d, $J = 7.0$ Hz,
898 Fmoc), 7.82.

899 ^{13}C -NMR (125 MHz, CDCl_3): δ 12.5 (CH_3 , Pbf), 17.9 (CH_3 , Pbf), 19.3 (CH_3 ,
900 Pbf), 25.5 ($\text{C}\gamma$), 28.6 (CH_3 , Pbf), 40.9 ($\text{C}\delta$), 43.2 (CH_2 , Pbf), 47.0 (CH , Fmoc),
901 59.1 (OCH_3), 60.3 (OCH_3), 60.5 (OCH_3), 67.3 (CH_2 , Fmoc), 70.3 (C_6), 74.8 (C_5),
902 77.4 (C_4), 83.5 (C_2), 85.0 (C_3), 86.4 (CH , Fmoc), 103.1 (C_1), 117.6 (arom. Pbf),
903 119.9 (arom. Fmoc), 124.7 (arom. Pbf), 125.2 (arom. Fmoc), 127.1 (arom. Fmoc),
904 127.7 (arom. Fmoc), 132.3 (arom. Pbf), 132.7 (arom. Pbf), 138.3 (arom. Pbf),
905 141.1 (arom. Fmoc), 143.7 (arom. Fmoc), 156.4 (arom. Pbf), 158.8 ($-\text{O}-\text{C}$ arom.
906 Pbf)

907 FT-IR (KBr): 3442, 2930, 2836, 1722, 1663, 1622, 1551, 1454, 1375, 1310,
908 1125, 1184, 951, 853, 812, 785, 761, 741 (Fmoc), 700, 662, 567 (Pbf, $-\text{SO}_2\text{NH}-$)
909 cm^{-1}

910

911 **1-(Tri-*O*-methylcellulosyl)-4-(L-arginine-L-arginine-*N*-methyl)-1*H*-1,2,3-**
912 **triazole (2b)**

913 1-(Tri-*O*-methylcellulosyl)-4-($N\alpha$ -Fmoc- $N\omega$ -Pbf-L-arginine- $N\omega$ -Pbf-L-
914 arginine-*N*-methyl)-1*H*-1,2,3-triazole (**5b**, 293 mg) was dissolved in
915 piperidine/dichloromethane (1/1, v/v, 4 mL). The reaction mixture was stirred at
916 room temperature for 4 h under nitrogen, after which it was concentrated and
917 purified by gel-filtration column chromatography (LH-60, eluent: 20%
918 MeOH/ CH_2Cl_2) to give 1-(tri-*O*-methylcellulosyl)-4-($N\omega$ -Pbf-L-arginine- $N\omega$ -Pbf-
919 L-arginine-*N*-methyl)-1*H*-1,2,3-triazole (260 mg, 89% yield; GPC analysis: $M_n =$
920 6.7×10^3 , $M_w / M_n = 1.7$).

921 1-(Tri-*O*-methylcellulosyl)-4-($N\omega$ -Pbf-L-arginine- $N\omega$ -Pbf-L-arginine-*N*-
922 methyl)-1*H*-1,2,3-triazole (244 mg) was dissolved in trifluoroacetic acid/distilled
923 water (1/4, v/v, 2 mL) and stirred at 37 °C for 4 h under nitrogen. The mixture

924 was concentrated, purified by gel-filtration column chromatography (LH-60,
925 eluent: 20% MeOH/CH₂Cl₂), and further purified by PTLC (eluent: 10%
926 MeOH/CH₂Cl₂). The purified 1-(tri-*O*-methyl-cellulosyl)-4-(L-arginine-L-
927 arginine-*N*-methyl)-1*H*-1,2,3-triazole was dispersed in water. Water-soluble
928 component was collected by removal of the water-insoluble component by
929 filtration through cotton wool, which was then concentrated to give 1-(tri-*O*-
930 methylcellulosyl)-4-(L-arginine-L-arginine-*N*-methyl)-1*H*-1,2,3-triazole (**2b**, 186
931 mg, 76% yield, GPC analysis: $M_n = 6.0 \times 10^3$, $M_w / M_n = 1.6$).

932 ¹H-NMR (500 MHz, D₂O): δ 1.5-2.0 (m, H_γ and H_{γ'}, H_β, H_{β'}), 3.13 (t, $J = 8.5$
933 Hz, H_{2_{Me}}), 3.40 (s, OMe), 3.45 (t, $J = 9.5$ Hz, H_{3_{Me}}), 3.56 (s, OMe), 3.58 (s, OMe),
934 3.55-3.60 (H_{5_{Me}}), 3.68-3.80 (H_{4_{Me}}, H_{6_{Me}}), 4.42 (d, $J = 7.5$ Hz, H_{1_{Me}}), 4.65 (d, $J =$
935 8.0 Hz), 4.99 (d, $J = 3.5$ Hz), 5.40 (d, $J = 3.5$ Hz), 5.62 (broad s), 8.42 (s, CH,
936 triazole)

937 FT-IR (KBr): 3446, 2922, 2836, 1624, 1456, 1375, 1314, 1125, 1078, 947, 768,
938 702, 662, 606, 581, 538, 488 cm⁻¹

939

940 **1-(Tri-*O*-methyl-cellulosyl)-4-[Fmoc-Glu(*O**t*-Bu)-Glu(*O**t*-Bu)-*N*-methyl]-**
941 **1*H*-1,2,3-triazole (6b)**

942 Sodium ascorbate (109 mg/137 μL, 0.55 mmol, 20 equiv., 4 M in H₂O) and
943 CuSO₄·5H₂O (68 mg, MW = 249.69, 0.27 mmol, 10 equiv.) were added to a
944 solution of *N*α-Fmoc-Glu(*O**t*-Bu)-Glu(*O**t*-Bu)-*N*-propargylamide (**10**, 53 mg,
945 MW = 647.77, 0.082 mmol, 3.0 equiv.) and tri-*O*-methylcellulosyl azide (**7b**, 200
946 mg, $M_n = 7.34 \times 10^3$, $DP_n = 35.8$, 0.027 mmol, 1.0 equiv.) in
947 methanol/dichloromethane (1/4, v/v, 5 mL). The reaction mixture was stirred at
948 room temperature for 14 h under nitrogen, after which it was concentrated and

949 passed through a silica-gel chromatography column (eluent: 20% MeOH/CH₂Cl₂).
950 The crude product was purified by gel-filtration column chromatography (LH-60,
951 eluent: 20% MeOH/CH₂Cl₂), and then by PTLC (eluent: 10% MeOH/CH₂Cl₂) to
952 give 1-(tri-*O*-methylcellulosyl)-4-[Fmoc-Glu(*O**t*-Bu)-Glu(*O**t*-Bu)-*N*-methyl]-1*H*-
953 1,2,3-triazole (186 mg, 93% yield, GPC analysis: $M_n = 7.4 \times 10^3$, $M_w / M_n = 1.6$).

954 ¹H-NMR (500 MHz, CDCl₃): δ 1.43 (s, CH₃ (*t*Bu)), 1.47 (s, CH₃ (*t*Bu)), 2.0-2.2
955 (m, 4H, H β), 2.25-2.450 (m, 4H, H γ), 2.96 (t, $J = 8.5$ Hz, H2_{Me}), 3.22 (t, $J = 9.0$ Hz,
956 H3_{Me}), 3.29 (m, H5_{Me}), 3.39 (s, OMe), 3.54 (s, OMe), 3.59 (s, OMe), 3.64-3.74
957 (H4_{Me}), 3.64-3.82 (H6_{Me}), 4.1-4.2 (1H, H α), 4.25-4.35 (2H, CH₂ (Fmoc)), 4.35 (d,
958 $J = 7.5$ Hz, H1_{Me}), 7.32 (t, $J = 7.5$ Hz, arom., Fmoc), 7.40 (t, $J = 7.5$ Hz, arom.,
959 Fmoc), 7.62 (broad d, $J = 7.0$ Hz, arom., Fmoc), 7.76 (d, $J = 7.5$ Hz, arom., Fmoc)

960 ¹³C-NMR (125 MHz, CDCl₃): δ 28.0 (CH₃ (*t*Bu)), 28.0 (CH₃ (*t*Bu)), 31.9
961 (triazole-CH₂-NH-C α -C β -C γ), 35.2 (triazole-CH₂-NH-), 47.1 (CH, Fmoc), 59.1
962 (OCH₃), 59.6, 60.1, 60.3 (OCH₃), 60.4, 60.5 (OCH₃), 60.8, 67.2 (CH₂, Fmoc),
963 70.3 (C6), 72.2, 73.2, 73.2, 74.9 (C5), 77.4 (C4), 81.2 (C(CH₃)₃), 83.5 (C2), 85.0
964 (C3), 86.1, 103.1 (C1), 120.0 (arom. Fmoc), 125.1 (arom. Fmoc), 127.1 (arom.
965 Fmoc), 127.7 (arom. Fmoc), 141.3 (arom. Fmoc), 143.8 (arom. Fmoc), 144.4
966 (arom. Fmoc)

967 FT-IR (KBr): 3430, 2932, 2904, 2836, 1728, 1672, 1514 (*t*Bu), 1454, 1373,
968 1312, 1125, 1084, 1059, 951, 889, 851, 762, 743 (Fmoc), 704, 656, 615, 577 cm⁻¹
969

970 **1-(Tri-*O*-methyl-cellulosyl)-4-(Glu-Glu-*N*-methyl)-1*H*-1,2,3-triazole (3b)**

971 1-(Tri-*O*-methyl-cellulosyl)-4-[Fmoc-Glu(*O**t*-Bu)-Glu(*O**t*-Bu)-*N*-methyl]-1*H*-
972 1,2,3-triazole (161 mg) was dissolved in piperidine/dichloromethane (1/1, v/v, 2
973 mL). The reaction mixture was stirred at room temperature for 4 h under nitrogen,

974 after which it was concentrated and purified by gel-filtration column
975 chromatography (LH-60, eluent: 20% MeOH/CH₂Cl₂), and then by PTLC (eluent:
976 10% MeOH/CH₂Cl₂) to give 1-(tri-*O*-methylcellulosyl)-4-[Glu(*O**t*-Bu)-Glu(*O**t*-
977 Bu)-*N*-methyl]-1*H*-1,2,3-triazole (136 mg, 84% yield; GPC analysis: $M_n =$
978 8.0×10^3 , $M_w / M_n = 1.6$).

979 1-(Tri-*O*-methylcellulosyl)-4-[Glu(*O**t*-Bu)-Glu(*O**t*-Bu)-*N*-methyl]-1*H*-1,2,3-
980 triazole (124 mg) was dissolved in trifluoroacetic acid/distilled water (9/1, v/v, 1
981 mL). The reaction mixture was stirred at room temperature for 4 h under nitrogen
982 atmosphere, concentrated, and then purified by gel-filtration column
983 chromatography (LH-60, eluent: 20% MeOH/CH₂Cl₂), and further purified by
984 PTLC) eluent: 10% MeOH/CH₂Cl₂). The water-soluble component was collected
985 by removal of the water-insoluble component by filtration, and concentrated to
986 give 1-(tri-*O*-methylcellulosyl)-4-(Glu-Glu-*N*-methyl)-1*H*-1,2,3-triazole (**3b**, 64
987 mg, 52% yield; GPC analysis: $M_n = 7.0 \times 10^3$, $M_w / M_n = 1.6$).

988 ¹H-NMR (500 MHz, D₂O): δ 3.14 (t, $J = 9.0$ Hz, H_{2_{Me}}), 3.40 (s, OMe), 3.45 (t, J
989 = 9.0 Hz, H_{3_{Me}}), 3.57 (s, OMe), 3.58 (s, OMe), 3.57-3.62 (H_{5_{Me}}), 3.60-3.82 (H_{4_{Me}},
990 H_{6_{Me}}), 4.43 (d, $J = 8.0$ Hz, H_{1_{Me}}), 4.48 (d, 5.40 (d, $J = 3.0$ Hz), $J = 3.5$ Hz), 5.43
991 (broad s), 8.43 (s, triazole *CH*)

992 FT-IR (KBr): 3460, 2928, 2836, 1732, 1626, 1458, 1377, 1310, 1126, 1084,
993 1061, 945, 800, 704, 664, 571, 486 cm⁻¹

994 **Characterization**

995 *General*

996 ¹H- and ¹³C-NMR spectra were recorded on a Varian 500 NMR (500 MHz) or
997 Varian INOVA300 (300 MHz) spectrometer in chloroform-*d* with
998 tetramethylsilane as the internal standard, or in deuterium oxide with 3-

999 (trimethylsilyl)-1-propanesulfonic acid sodium salt as the external standard.
1000 Chemical shifts (δ) and coupling constants (J) are given in ppm and Hz,
1001 respectively. Matrix-assisted laser-desorption/ionization time-of-flight mass
1002 spectrometry (MALDI-TOF MS) was performed on a Bruker MALDI-TOF
1003 Autoflex III mass spectrometer in positive ion and reflector or linear modes. A
1004 smartbeam laser was used for ionization. All spectra were acquired in linear mode
1005 and calibrated externally. 2,5-Dihydroxybenzoic acid was used as the matrix in
1006 MALDI-TOF MS experiments. Shimadzu components, namely the liquid
1007 chromatography injector (LC-10ATvp), column oven (CTO-10Avp), ultraviolet-
1008 visible detector (SPD-10Avp), refractive index detector (RID-10A),
1009 communication bus module (CBM-10A), and LC workstation (CLASS-LC10),
1010 were used for HPLC separations, with Shodex columns (KF802, KF802.5, and
1011 KF805). Number- and weight-averaged molecular weights (M_n , M_w) and
1012 polydispersity indices (M_w/M_n) were determined using polystyrene standards
1013 (Shodex). A flow rate of 1 mL/min at 40 °C was chosen, and chloroform was used
1014 as the eluent.

1015 *Differential scanning calorimetry (DSC)*

1016 DSC thermograms were recorded on a DSC823^e instrument (Mettler Toledo,
1017 Zurich, Switzerland) with an HSS7 sensor under nitrogen during (0 → 90 → 0 °C)
1018 heating/cooling cycles, with heating and cooling rates of 3.5 °C/min. Each
1019 temperature cycle was repeated three times in order to ensure reproducibility.
1020 Sample concentrations of 2.0 wt% were used in DSC experiments.

1021 *Dynamic light scattering (DLS) experiments*

1022 DLS experiments were performed with an ELS-Z zeta-potential and particle-
1023 size analyzer (Otsuka Electronics Co., Ltd, Osaka, Japan) and conducted in the

1024 10–90 °C temperature range. Sample solutions were maintained at the required
1025 temperature for 5 min prior to each experiment. Sample concentrations of 0.2 wt%
1026 were used in these experiments.

1027 *Surface-tension measurements*

1028 Surface tensions were measured with a CBVP-A3 surface tensiometer (Kyowa
1029 Interface Science, Co. Ltd., Tokyo, Japan) at 23 °C using the Wilhelmy method.
1030 A Teflon cell containing 700 µL of the required solution was used in these
1031 experiments. Surface tensions gradually decreased with time, and stable values
1032 were recorded after 30 min.

1033 *Scanning electron microscopy (SEM) and transmission electron* 1034 *microscopy (TEM)*

1035 The three hydrogels from aqueous solutions containing compounds **1b**, **2b**, and
1036 **3b** were frozen in liquid nitrogen, lyophilized, and cut with a razor blade. The cut
1037 surfaces of the hydrogels were sputter-coated with gold with an ion-coater (JFC-
1038 1100E, JEOL, Tokyo, Japan) and examined by scanning electron microscopy
1039 (SEM, JSM-6060, JEOL) at an accelerator voltage of 5 kV.

1040 A drop of an aqueous dispersion of compound **2b** was mounted on a copper grid
1041 with an elastic carbon-support film (Oken Shoji, Tokyo, Japan) and examined by
1042 transmission electron microscopy (TEM, JEM1400, JEOL) at an accelerator
1043 voltage of 100 kV after negative staining with uranyl acetate.

1044 *Release of model drugs from the thermoresponsive hydrogels*

1045 Compounds **2b** and **3b** (2 or 4 mg) were respectively added to glass vials
1046 containing solutions of diclofenac sodium (DFNa) or imipramine hydrochloride
1047 (IMC) (0.025 wt%) in PBS (100 µL), and the compounds were dissolved at about
1048 0 °C. The glass vial was then heated at 37 °C for 10 min while left to stand. After

1049 a hydrogel had formed, a fresh PBS solution (500 μ L), which had been pre-heated
1050 to 37 $^{\circ}$ C, was carefully poured onto the hydrogel surface. The glass vial was
1051 shaken at 60 rpm in a water-bath shaker (Eyela NTS-4000, Tokyo Rikakikai Co.,
1052 Ltd.). The aqueous layer (500 μ L) was then collected and filtered through a
1053 membrane filter (pore size: 0.45 μ m). The UV absorbance of the aqueous solution
1054 was recorded at 260 nm in a 96-well microplate using a SpectraMax Plus 384
1055 Microplate Reader (Molecular Devices). The amount of released drug was
1056 evaluated from the UV absorbance.

1057 *Cytotoxicity assays*

1058 Compounds **1b**, **2b**, and **3b** were dispersed in PBS at a concentration of 20
1059 mg/mL and serially diluted by factors of two in a 96-well flat-bottomed plate (50
1060 μ L/well (Corning Inc., Corning, NY). The human histiocytoma U937 cell line was
1061 suspended in complete RPMI1640 medium at 1×10^4 cells/mL and the cell
1062 suspension was added to the 96-well flat bottom plate (5×10^2 cells/50 μ l/well).
1063 The plate was incubated at 37 $^{\circ}$ C in a 5%-CO₂ atmosphere for 4 d. The plate was
1064 allowed to stand at room temperature for 30 min, after which 100 μ L of CellTiter-
1065 Glo Luminescent Cell Viability Assay reagent (Promega Corp., Madison, WI)
1066 was added to each well. After thorough mixing, the contents of each well were
1067 transferred into an OptiplateTM-96 multi-well plate (Perkin Elmer, Waltham, MA).
1068 Cell viability was determined by measuring luminescence with an ARVOTM SX
1069 Delfia 1420 Multilabel Counter (Perkin Elmer Life and Analytical Sciences,
1070 Shelton, CT).

1071

1072 **Acknowledgements** This work was supported in part by JSPS Grants-in-Aid for Scientific
1073 Research (B) nos. 24380092 and 15H04531.

1074

1075

1076 **References**

- 1077 Aagren JKM, Billing JF, Grundberg HE, Nilsson UJ (2006) Synthesis of a chiral and fluorescent
1078 sugar-based macrocycle by 1,3-dipolar cycloaddition *Synthesis*:3141-3145 doi:10.1055/s-
1079 2006-942503
- 1080 Akiyoshi K, Kohara M, Ito K, Kitamura S, Sunamoto J (1999) Enzymic synthesis and
1081 characterization of amphiphilic block copolymers of poly(ethylene oxide) and amylose
1082 *Macromol Rapid Commun* 20:112-115 doi:10.1002/(SICI)1521-
1083 3927(19990301)20:3<112::AID-MARC112>3.0.CO;2-Q
- 1084 Baumann MD, Kang CE, Stanwick JC, Wang Y, Kim H, Lapitsky Y, Shoichet MS (2009) An
1085 injectable drug delivery platform for sustained combination therapy *J Controlled Release*
1086 138:205-213 doi:10.1016/j.jconrel.2009.05.009
- 1087 Bodvik R et al. (2010) Aggregation and network formation of aqueous methylcellulose and
1088 hydroxypropylmethylcellulose solutions *Colloids Surf, A* 354:162-171
1089 doi:10.1016/j.colsurfa.2009.09.040
- 1090 Bonduelle C, Lecommandoux S (2013) Synthetic Glycopolypeptides as Biomimetic Analogues of
1091 Natural Glycoproteins *Biomacromolecules* 14:2973-2983 doi:10.1021/bm4008088
- 1092 Breitenbach BB, Schmid I, Wich PR (2017) Amphiphilic Polysaccharide Block Copolymers for
1093 pH-Responsive Micellar Nanoparticles *Biomacromolecules* 18:2839-2848
1094 doi:10.1021/acs.biomac.7b00771
- 1095 Dax D, Xu C, Langvik O, Hemming J, Backman P, Willfoer S (2013) Synthesis of SET-LRP-
1096 induced galactoglucomannan-diblock copolymers *J Polym Sci, Part A: Polym Chem*
1097 51:5100-5110 doi:10.1002/pola.26942
- 1098 de Medeiros Modolon S, Otsuka I, Fort S, Minatti E, Borsali R, Halila S (2012) Sweet Block
1099 Copolymer Nanoparticles: Preparation and Self-Assembly of Fully Oligosaccharide-
1100 Based Amphiphile *Biomacromolecules* 13:1129-1135 doi:10.1021/bm3000138
- 1101 Desbrieres J, Hirrien M, Rinaudo M (1998) A calorimetric study of methylcellulose gelation
1102 *Carbohydr Polym* 37:145-152
- 1103 Du X, Zhou J, Shi J, Xu B (2015) Supramolecular Hydrogelators and Hydrogels: From Soft Matter
1104 to Molecular Biomaterials *Chemical Reviews* 115:13165-13307
1105 doi:10.1021/acs.chemrev.5b00299
- 1106 Fajardo AR, Guerry A, Britta EA, Nakamura CV, Muniz EC, Borsali R, Halila S (2014) Sulfated
1107 Glycosaminoglycan-Based Block Copolymer: Preparation of Biocompatible Chondroitin
1108 Sulfate-b-poly(lactic acid) Micelles *Biomacromolecules* 15:2691-2700
1109 doi:10.1021/bm5005355
- 1110 Fundueanu G, Constantin M, Ascenzi P (2009) Poly(N-isopropylacrylamide-co-acrylamide) cross-
1111 linked thermoresponsive microspheres obtained from preformed polymers: influence of
1112 the physico-chemical characteristics of drugs on their release profiles *Acta Biomater*
1113 5:363-373 doi:10.1016/j.actbio.2008.07.011
- 1114 Heymann E (1935) Studies on sol-gel transitions. 1. The inverse sol-gel transformation of
1115 methylcellulose in water *Trans Faraday Soc* 31:846
- 1116 Hung C-C et al. (2017) Conception of Stretchable Resistive Memory Devices Based on
1117 Nanostructure-Controlled Carbohydrate-block-Polyisoprene Block Copolymers *Adv*
1118 *Funct Mater* 27:n/a doi:10.1002/adfm.201606161
- 1119 Kamitakahara H, Baba A, Yoshinaga A, Suhara R, Takano T (2014) Synthesis and crystallization-
1120 induced microphase separation of cellulose triacetate-block-poly(γ -benzyl-L-glutamate)
1121 *Cellulose (Dordrecht, Neth)* 21:3323-3338 doi:10.1007/s10570-014-0383-3
- 1122 Kamitakahara H, Funakoshi T, Nakai S, Takano T, Nakatsubo F (2009a) Syntheses of 6-O-
1123 ethyl/methyl-celluloses via ring-opening copolymerization of 3-O-benzyl-6-O-
1124 ethyl/methyl-alpha-d-glucopyranose 1,2,4-orthopivalates and their structure-property
1125 relationships *Cellulose* 16:1179-1185 doi:Doi 10.1007/S10570-009-9339-4
- 1126 Kamitakahara H, Funakoshi T, Takano T, Nakatsubo F (2009b) Syntheses of 2,6-O-alkyl
1127 celluloses: Influence of methyl and ethyl groups regioselectively introduced at O-2 and
1128 O-6 positions on their solubility *Cellulose* 16:1167-1178
- 1129 Kamitakahara H, Koschella A, Mikawa Y, Nakatsubo F, Heinze T, Klemm D (2008a) Syntheses
1130 and comparison of 2,6-di-O-methyl celluloses from natural and synthetic celluloses
1131 *Macromolecular Bioscience* 8:690-700

- 1132 Kamitakahara H, Murata-Hirai K, Tanaka Y (2012) Synthesis of blockwise alkylated
1133 tetrasaccharide-organic quantum dot complexes and their utilization for live cell labeling
1134 with low cytotoxicity *Cellulose* 19:171-187 doi:Doi 10.1007/S10570-011-9619-7
- 1135 Kamitakahara H, Nakatsubo F (2010) ABA- and BAB-triblock cooligomers of tri-O-methylated
1136 and unmodified cello-oligosaccharides: syntheses and structure-solubility relationship
1137 *Cellulose* 17:173-186 doi:Doi 10.1007/S10570-009-9348-3
- 1138 Kamitakahara H, Nakatsubo F, Klemm D (2006) Block co-oligomers of tri-O-methylated and
1139 unmodified cello-oligosaccharides as model compounds for methylcellulose and its
1140 dissolution/gelation behavior *Cellulose* 13:375-392
- 1141 Kamitakahara H, Nakatsubo F, Klemm D (2007) New class of carbohydrate-based nonionic
1142 surfactants: diblock co-oligomers of tri-O-methylated and unmodified cello-
1143 oligosaccharides *Cellulose* 14:513-528
- 1144 Kamitakahara H, Nakatsubo F, Klemm D (2009c) Synthesis of methylated cello-oligosaccharides:
1145 synthesis strategy for block-wise methylated cello-oligosaccharides *ACS Symp Ser*
1146 1017:199-211 doi:10.1021/bk-2009-1017.ch011
- 1147 Kamitakahara H, Suhara R, Yamagami M, Kawano H, Okanishi R, Asahi T, Takano T (2016) A
1148 versatile pathway to end-functionalized cellulose ethers for click chemistry applications
1149 *Carbohydr Polym* 151:88-95 doi:10.1016/j.carbpol.2016.05.016
- 1150 Kamitakahara H, Yoshinaga A, Aono H, Nakatsubo F, Klemm D, Burchard W (2008b) New
1151 approach to unravel the structure-property relationship of methylcellulose. Self-assembly
1152 of amphiphilic block-like methylated cello-oligosaccharides *Cellulose* 15:797-801
1153 doi:10.1007/s10570-008-9232-6
- 1154 Karakawa M, Mikawa Y, Kamitakahara H, Nakatsubo F (2002) Preparations of regioselectively
1155 methylated cellulose acetates and their H-1 and C-13 NMR spectroscopic analyses *J*
1156 *Polym Sci Pol Chem* 40:4167-4179
- 1157 Kato T, Yokoyama M, Takahashi A (1978) Melting temperatures of thermally reversible gels
1158 *Colloid Polym Sci* 256:15-21
- 1159 Kunishima M, Kawachi C, Iwasaki F, Terao K, Tani S (1999a) Synthesis and characterization of
1160 4-(4,6-dimethoxy-1,3,5-triazin-2-yl)-4-methylmorpholinium chloride *Tetrahedron Lett*
1161 40:5327-5330 doi:10.1016/S0040-4039(99)00968-5
- 1162 Kunishima M, Kawachi C, Morita J, Terao K, Iwasaki F, Tani S (1999b) 4-(4,6-Dimethoxy-1,3,5-
1163 triazin-2-yl)-4-methylmorpholinium chloride: an efficient condensing agent leading to the
1164 formation of amides and esters *Tetrahedron* 55:13159-13170 doi:10.1016/S0040-
1165 4020(99)00809-1
- 1166 Liu J-Y, Zhang L-M (2007) Preparation of a polysaccharide-polyester diblock copolymer and its
1167 micellar characteristics *Carbohydr Polym* 69:196-201 doi:10.1016/j.carbpol.2006.09.009
- 1168 Loos K, Müller AHE (2002) New Routes to the Synthesis of Amylose-block-polystyrene Rod-
1169 Coil Block Copolymers *Biomacromolecules* 3:368-373 doi:10.1021/bm0156330
- 1170 Lott JR, McAllister JW, Arvidson SA, Bates FS, Lodge TP (2013a) Fibrillar Structure of
1171 Methylcellulose Hydrogels *Biomacromolecules* 14:2484-2488 doi:10.1021/bm400694r
- 1172 Lott JR, McAllister JW, Wasbrough M, Sammler RL, Bates FS, Lodge TP (2013b) Fibrillar
1173 Structure in Aqueous Methylcellulose Solutions and Gels *Macromolecules (Washington,*
1174 *DC, U S)* 46:9760-9771 doi:10.1021/ma4021642
- 1175 Morelli P, Matile S (2017) Sidechain Engineering in Cell-Penetrating Poly(disulfide)s *Helv Chim*
1176 *Acta* 100:e1600370 doi:10.1002/hlca.201600370
- 1177 Nakagawa A, Fenn D, Koschella A, Heinze T, Kamitakahara H (2011a) Physical Properties of
1178 Diblock Methylcellulose Derivatives with Regioselective Functionalization Patterns: First
1179 Direct Evidence that a Sequence of 2,3,6-Tri-O-methyl-glucofuranosyl Units Causes
1180 Thermoreversible Gelation of Methylcellulose *Journal of Polymer Science Part B-*
1181 *Polymer Physics* 49:1539-1546 doi:Doi 10.1002/Polb.22343
- 1182 Nakagawa A, Fenn D, Koschella A, Heinze T, Kamitakahara H (2011b) Synthesis of Diblock
1183 Methylcellulose Derivatives with Regioselective Functionalization Patterns *J Polym Sci*
1184 *Pol Chem* 49:4964-4976 doi:Doi 10.1002/Pola.24952
- 1185 Nakagawa A, Ishizu C, Sarbova V, Koschella A, Takano T, Heinze T, Kamitakahara H (2012a) 2-
1186 O-Methyl- and 3,6-Di-O-methyl-cellulose from Natural Cellulose: Synthesis and
1187 Structure Characterization *Biomacromolecules* 13:2760-2768 doi:Doi
1188 10.1021/Bm300754u
- 1189 Nakagawa A, Kamitakahara H, Takano T (2011c) Synthesis of blockwise alkylated (1->4) linked
1190 trisaccharides as surfactants: influence of configuration of anomeric position on their
1191 surface activities *Carbohydr Res* 346:1671-1683 doi:10.1016/j.carres.2011.04.034

- 1192 Nakagawa A, Kamitakahara H, Takano T (2012b) Synthesis and thermoreversible gelation of
 1193 diblock methylcellulose analogues via Huisgen 1,3-dipolar cycloaddition *Cellulose*
 1194 19:1315-1326 doi:Doi 10.1007/S10570-012-9703-7
- 1195 Nakagawa A, Steiniger F, Richter W, Koschella A, Heinze T, Kamitakahara H (2012c)
 1196 Thermoresponsive Hydrogel of Diblock Methylcellulose: Formation of Ribbonlike
 1197 Supramolecular Nanostructures by Self-Assembly *Langmuir* 28:12609-12618
- 1198 Otsuka I, Osaka M, Sakai Y, Travelet C, Putaux J-L, Borsali R (2013) Self-Assembly of
 1199 Maltoheptaose-block-Polystyrene into Micellar Nanoparticles and Encapsulation of Gold
 1200 Nanoparticles *Langmuir* 29:15224-15230 doi:10.1021/la403941v
- 1201 Otsuka I, Travelet C, Halila S, Fort S, Pignot-Paintrand I, Narumi A, Borsali R (2012)
 1202 Thermoresponsive Self-Assemblies of Cyclic and Branched Oligosaccharide-block-
 1203 poly(N-isopropylacrylamide) Diblock Copolymers into Nanoparticles
 1204 *Biomacromolecules* 13:1458-1465 doi:10.1021/bm300167e
- 1205 Parker J, Mitrousis N, Shoichet MS (2016) Hydrogel for Simultaneous Tunable Growth Factor
 1206 Delivery and Enhanced Viability of Encapsulated Cells in Vitro *Biomacromolecules*
 1207 17:476-484 doi:10.1021/acs.biomac.5b01366
- 1208 Rees DA (1972) Polysaccharide gels, A molecular view *Chem & Ind (London)* 19:630-636
- 1209 Sakai-Otsuka Y, Zaioncz S, Otsuka I, Halila S, Rannou P, Borsali R (2017) Self-Assembly of
 1210 Carbohydrate-block-Poly(3-hexylthiophene) Diblock Copolymers into Sub-10 nm Scale
 1211 Lamellar Structures *Macromolecules* 50:3365-3376 doi:10.1021/acs.macromol.7b00118
- 1212 Savage AB (1957) Temperature-Viscosity Relationships for Water-Soluble Cellulose Ethers *Ind*
 1213 *Eng Chem* 49:99
- 1214 Schamann M, Schafer HJ (2003) TEMPO-mediated anodic oxidation of methyl glycosides and 1-
 1215 methyl and 1-azido disaccharides *Eur J Org Chem*:351-358 doi:10.1002/ejoc.200390041
- 1216 Togashi D, Otsuka I, Borsali R, Takeda K, Enomoto K, Kawaguchi S, Narumi A (2014)
 1217 Maltopentaose-Conjugated CTA for RAFT Polymerization Generating Nanostructured
 1218 Bioresource-Block Copolymer *Biomacromolecules* 15:4509-4519
 1219 doi:10.1021/bm501314f
- 1220 Yagi S, Kasuya N, Fukuda K (2010) Synthesis and characterization of cellulose-b-polystyrene
 1221 *Polym J (Tokyo, Jpn)* 42:342-348 doi:10.1038/pj.2009.342
- 1222 Yamagami M, Kamitakahara H, Yoshinaga A, Takano T (2018) Thermo-reversible
 1223 supramolecular hydrogels of trehalose-type diblock methylcellulose analogues *Carbohydr*
 1224 *Polym* 183:110-122 doi:10.1016/j.carbpol.2017.12.006
- 1225 Yang HW, Yi JW, Bang E-K, Jeon EM, Kim BH (2011) Cationic nucleolipids as efficient siRNA
 1226 carriers *Org Biomol Chem* 9:291-296 doi:10.1039/C0OB00580K
- 1227 Ying LQ, Gervay-Hague J (2003) General methods for the synthesis of glycopyranosyluronic acid
 1228 azides *Carbohydr Res* 338:835-841 doi:10.1016/S0008-6215(03)00042-9
- 1229 Yu G-J, Chen X-Y, Mao S-Z, Liu M-L, Du Y-R (2017) Hydrophobic terminal group of surfactant
 1230 initiating micellization as revealed by 1H NMR spectroscopy *Chin Chem Lett* 28:1413-
 1231 1416 doi:10.1016/j.ccllet.2017.04.013

1232